Cellular Microbiology (2006) 8(5), 806–814

doi:10.1111/j.1462-5822.2005.00667.x
First published online 21 December 2005

The ability to form biofilm influences *Mycobacterium avium* invasion and translocation of bronchial epithelial cells

Yoshitaka Yamazaki,[1] Lia Danelishvili,[1] Martin Wu,[1] Eiko Hidaka,[2] Tsutomu Katsuyama,[2] Bernadette Stang,[1] Mary Petrofsky,[3] Robert Bildfell[1] and Luiz E. Bermudez[1,4]*

[1]*Department of Biomedical Sciences, College of Veterinary Medicine, and* [4]*Department of Microbiology, College of Science, Oregon State University, Corvallis, OR 97331, USA.*

[2]*Department of Laboratory Medicine, Sinshu University School of Medicine, 3-1-1 Asahi, Matsumoto, 390-8621 Japan.*

[3]*Kuzell Institute, California Pacific Medical Center Research Institute, San Francisco, CA 97115, USA.*

Summary

Organisms of the *Mycobacterium avium* complex (MAC) are widely distributed in the environment, form biofilms in water pipes and potable water tanks, and cause chronic lung infections in patients with chronic obstructive pulmonary disease and cystic fibrosis. Pathological studies in patients with pulmonary MAC infection revealed granulomatous inflammation around bronchi and bronchioles. BEAS-2B human bronchial epithelial cell line was used to study MAC invasion. MAC strain A5 entered polarized BEAS-2B cells with an efficiency of 0.1 ± 0.03% in 2 h and 11.3 ± 4.0% in 24 h. In contrast, biofilm-deficient transposon mutants 5G4, 6H9 and 9B5 showed impaired invasion. Bacteria exposed to BEAS-2B cells for 24 h had greater ability to invade BEAS-2B cells compared with bacteria incubated in broth. *M. avium* had no impact on the monolayer transmembrane resistance. Scanning electron microscopy showed that MAC A5 forms aggregates on the surface of BEAS-2B cell monolayers, and transmission electron microscopy evidenced MAC within vacuoles in BEAS-2B cells. Cells infected with the 5G4 mutant, however, showed significantly fewer bacteria and no aggregates on the cell surface. Mutants had impaired ability to cause infection in mice, as well. The ability to form biofilm appeared to be associated with the invasiveness of MAC A5.

Received 16 June, 2005; revised 6 October, 2005; accepted 27 October, 2005. *For correspondence. E-mail Luiz.Bermudez@oregonstate.edu; Tel. (+1) 541 737 6538; Fax (+1) 541 737 2730.

Introduction

Mycobacterium avium is widely distributed in the environment, being isolated from water and soil (Inderlied *et al.*, 1993; Primm *et al.*, 2004). *M. avium* is also a component of biofilms, and the urban water system has been shown to contain the bacterium on pipe surfaces (Benson and Ellner, 1993). *M. avium* infects AIDS patients, as well as individuals with chronic lung conditions, such as bronchiectasis, emphysema and cystic fibrosis (Aksamit, 2002; Ebert and Olivier, 2002). Recently, an increase in the incidence of *M. avium* infection has been documented in patients without predisposing lung pathology or AIDS (Prince *et al.*, 1989; Reich and Johnson, 1991). Bronchus and bronchioles are mainly affected, leading to thickness of the walls of the airways and formation of granulomas in the peribronchiolar region. This group of patients usually evolves to develop bronchiectasis, a pathological picture quite different from what is seen in tuberculosis (Reich and Johnson, 1991; Fujita *et al.*, 1999).

It has been suggested that the location of the *M. avium* granuloma in the peribronchiolar space would be secondary to the crossing of the bronchiolar mucosa, or alternatively, the bacterium would spread from the alveolar space through the lymphatic system. Recent work has demonstrated that *M. avium* can bind to human bronchial epithelium by interacting with the β_1 integrin, the fibronectin receptor (Middleton *et al.*, 2000). *M. avium*, as with many other pathogenic mycobacteria, can bind to fibronectin through the fibronectin attachment protein and the antigen 85 (Abou-Zeid *et al.*, 1988; Schorey *et al.*, 1996).

One of the major problems associated with chronic lung infection by *M. avium* is the limited response to therapy (Griffith *et al.*, 1998; 2000). Many of the patients either respond partially to treatment or develop resistance to the used antimicrobial, suggesting that biofilms may be associated with the infection. Recently, Carter *et al.* (2004) demonstrated that clarithromycin, but not moxifloxacin, can inhibit *M. avium* when used early in the biofilm formation process, but clarithromycin is ineffective when

employed on established biofilms, indicating that *M. avium* in biofilms is resistant to antibiotics (Carter *et al.*, 2004).

Our hypothesis is that *M. avium* can form biofilm in the bronchiolar and bronchial mucosa, protecting itself from the immune response, and subsequently cross the mucosal cells of the bronchiolar or bronchial airways. Once in the peribronchiolar space, it triggers the host response with consequent formation of granuloma. *Mycobacterium smegmatis*, as *M. avium*, establishes biofilm on solid surfaces, and previous studies have shown that the glycopeptidolipid (GPL) structure of the cell wall is associated with the ability to form biofilm (Recht and Kolter, 2001; Carter *et al.*, 2003; Yamazaki *et al.*, 2006). The inactivation of the GPL transport genes in *M. smegmatis* or the genes involved in the GPL biosynthesis in *M. avium* resulted in significant impairment of the bacteria's ability to form biofilm on PVC surfaces (Recht and Kolter, 2001; Yamazaki *et al.*, 2006).

To investigate whether biofilm is linked with the ability to infect and translocate across the bronchiolar and bronchial mucosa, we comparatively studied the behaviour of the wild-type *M. avium* strains and biofilm-deficient isogenic mutants *in vitro* and *in vivo*.

Results

Mycobacterium avium *invasion of BEAS-2B cell monolayer*

To characterize the ability of *M. avium* strains to enter bronchiolar epithelial cells, we used the strains MAC104, MAC101 and MAC A5. While the uptake at the 2 h time point was small, after 24 h, MAC104, MAC101 and MAC A5 strains were able to enter bronchiolar cells in a significant manner. Figure 1 shows the data obtained with MAC104 (similar to MAC101) and MAC A5. When the assay was repeated using three isogenic clones of MAC strain A5 (5G4, 6H9 and 9B5) which have significant impairment of the ability to form biofilm, it was observed that all three mutants failed to enter the epithelial cells in a similar fashion as the wild-type strain (Fig. 1). After 48 h, the efficiency of invasion did not differ significantly from the one observed after 24 h (data not shown). The complemented clones of the mutants 5G4, 6H9 and 9B5 were then examined in the invasion assay, in parallel with the biofilm-impaired mutants. As shown in Fig. 2, complementation of the gene function was associated with restoration of the capability to invade bronchiolar epithelial cells to a level comparable to the wild-type A5.

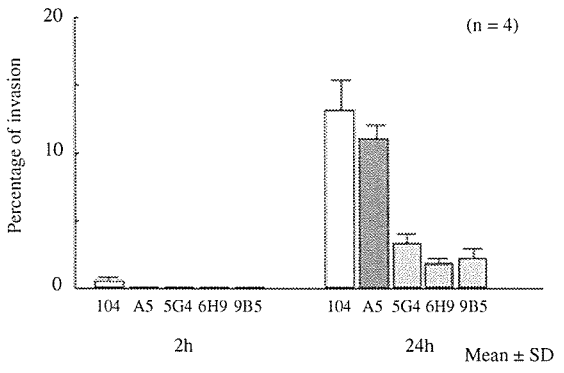

Fig. 1. Invasion of BEAS-2B human bronchiolar epithelial cells by *M. avium* strains 104 and A5, as well as biofilm-deficient strains, A5 isogenic mutants, 5G4, 6H9 and 9B5. $P < 0.05$ for the comparison between the wild-type strains and the mutants at 24 h.

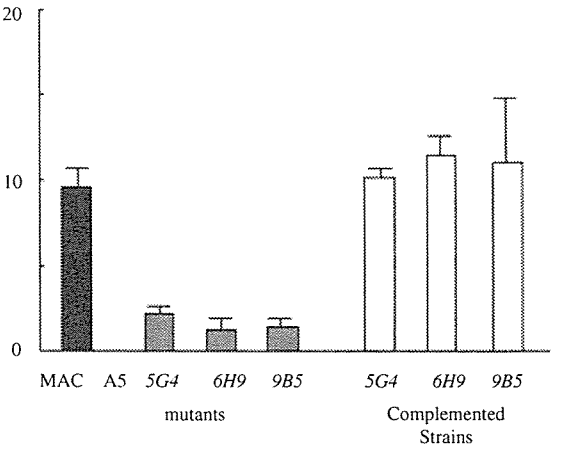

Fig. 2. Invasion assay (24 hr) comparing A5 strain with the isogenic mutants 5G4, 6H9 and 9B5 and the complemented strains. The results indicate recovery of the invasive phenotype by the complementation of the genes (Ma1565, 5G4; Ma*suc*A, 6H9; and Ma*pcd*, 9B5).

Scanning and transmission electron microscopy

Polarized monolayers on transwell membranes were used for these studies. Figure 3A and B shows electron micrographs of MAC104 and MAC A5 strains in contact with polarized BEAS-2B cells at 2 h. MAC104 (Fig. 3A) can be seen invading the epithelial cells with evident 'ruffles' at the point of entry, once again confirming the role of activation of Cdc42 in the interaction (Dam *et al.*, 2006). Interestingly, fine fibres, resembling fimbria-like structures, are also observed surrounding the bacteria. The strain A5 (Fig. 3B) can be observed forming aggregates on the cell surface. At the 24 h time point, both MAC104 (Fig. 3C) and MAC A5 (Fig. 3D) show evidence of forming biofilms. In contrast, the strain 5G4 is sparse and lacking biofilm formation at the same time point (Fig. 3E). In Fig. 3F, MAC104 strain is shown by transmission electron microscopy inside cytoplasmic vacuoles.

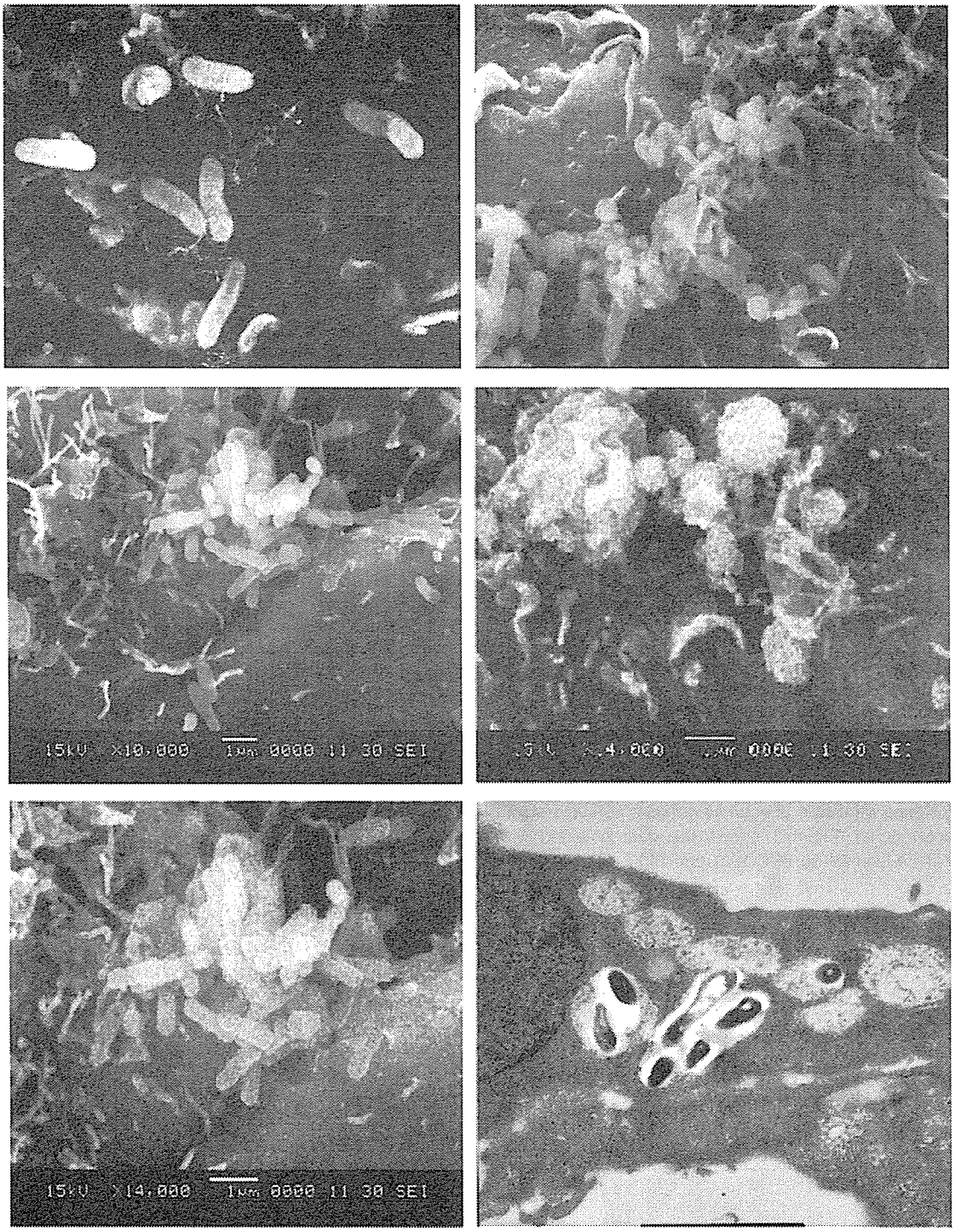

Fig. 3. Electron micrographs of *M. avium* invading polarized monolayers of BEAS-2B bronchiolar epithelial cells. Top left: MAC104 strain after 2 h, bacteria are seen entering host cells with 'ruffles'. Top right: strain A5 after 2 h of contact with BEAS-2B cells. Middle left and right: strain 104 and A5, after 24 h. Evidence of biofilm formation. Bottom left: strain 5G4 after 24 h in contact with epithelial cells. Of note is the lack of biofilm. Bottom right: transmission electron microscopy of MAC104 inside cytoplasmic vacuoles.

Table 1. Translocation of *M. avium* across polarized BEAS-2B bronchial epithelial cells.

	% of inoculum that translocated[a]					
M. avium strains	2 h	4 h	8 h	1 day	2 days	5 days
MAC104	0	0.3 ± 0.05	0.4 ± 0.02	0.8 ± 0.03	0.9 ± 0.02	1.1 ± 0.10
MAC A5	0	0.3 ± 0.02	0.4 ± 0.01	0.6 ± 0.02	0.7 ± 0.03	0.6 ± 0.03

a. The numbers represent the mean ± SD that crossed the barrier in the period of time between two time points. The experiment was repeated twice. There are no significant differences between the two strains at the same time point.

Translocation of M. avium

To determine whether *M. avium* was capable of translocating across polarized monolayers of BEAS-2B bronchiolar epithelial cells, both MAC104 and MAC A5 were exposed to impermeable monolayers. As observed in Table 1, *M. avium* translocated across BEAS-2B cells with a significant number of bacteria recovered from the bottom chamber after 4 h of infection. The number of cells that crossed the epithelial barrier was significantly greater after 24 h.

Effect of supernatant on bacterial invasion

As it was observed that invasion significantly increased from 2 h to 24 h of incubation in the presence of bronchiolar cells, and it was apparently associated with the ability to form biofilm, we sought to examine whether the supernatant of *M. avium* incubated with polarized BEAS-2B cells for 24 h had any effect on invasion. Bacteria in contact with BEAS-2B bronchiolar cells for 24 h were also obtained. It was observed that bacteria exposed to polarized monolayer of BEAS-2B for 24 h acquired an invasive phenotype and was able to enter fresh monolayers after 2 h of incubation; however, the supernatant had no effect on the invasion of epithelial cells. In contrast to the wild-type MAC104 and MAC A5 strains, the biofilm-deficient 5G4 strain in contact with BEAS-2B cells for 24 h did not express the invasive phenotype (Fig. 4).

Role of β1 integrin on invasion

Previous study has suggested that the β1 integrin fibronectin receptor was associated with the uptake of *M. avium* by the bronchial epithelium (Middleton *et al.*, 2000). In order to investigate the role of the β1 integrin in our model, we carried out the invasion assay of BEAS-2B bronchiolar epithelial cells in the presence of increasing concentrations of anti-β1 integrin antibody. Our results show that anti-β1 antibody at concentrations smaller than 100 μg ml^{-1} had no effect on the uptake of the MAC strain A5 by BEAS-2B cells after 24 h of incubation. In contrast, the use of β1 antibody inhibited the uptake of the strain MAC104 in a significant manner at the concentration of 100 μg ml^{-1} (Fig. 5). Non-specific antibody mouse IgG 2b had no effect on the uptake (data not shown).

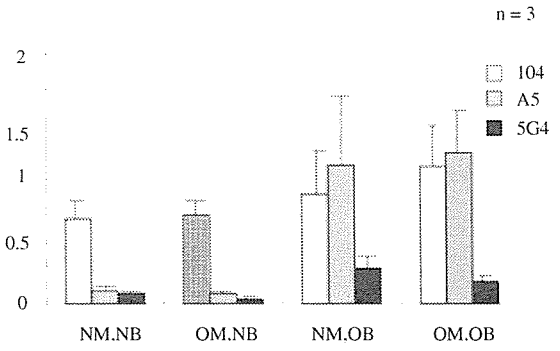

Fig. 4. Invasion of BEAS-2B epithelial cells by *M. avium*. Mycobacteria were incubated (OB) or not (NB) in the presence of BEAS-2B bronchiolar epithelial cells for 24 h, retrieved and used in a 2 h invasion assay. Supernatant of a 24 h incubation of bacteria with BEAS-2B cells was also used in combination with OB and NB. NM, new medium; OM, old medium. $P < 0.05$ for the comparisons between wild-type OB and NB; $P = 0.09$ for the comparisons between mutant OB and NB; $P = 0.1$ for all other comparisons.

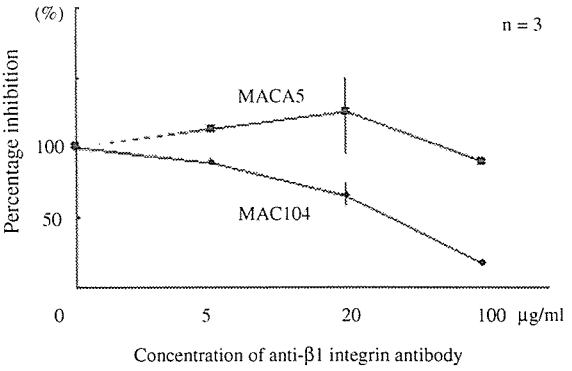

Fig. 5. The ability of anti-β1 integrin antibody to inhibit the *M. avium* uptake by BEAS-2B epithelial cells.

Table 2. Bacterial load in lung, liver and spleen of C57BL/6 mice infected intranasally with strain 101 of *M. avium*.

Time point (days)	Mean per organ ± SD[a]		
	Liver	Spleen	Lung
15	$9.3 \pm 0.4 \times 10^{1}$	$1.9 \pm 0.3 \times 10^{3}$	$9.7 \pm 0.2 \times 10^{3}$
30	$1.3 \pm 0.2 \times 10^{5}$	$1.4 \pm 0.2 \times 10^{5}$	$4.6 \pm 0.5 \times 10^{6}$
60	$3.5 \pm 0.2 \times 10^{5}$	$3.8 \pm 0.5 \times 10^{6}$	$3.3 \pm 0.4 \times 10^{7}$
90	$2.3 \pm 0.5 \times 10^{5}$	$5.8 \pm 0.9 \times 10^{6}$	$5.3 \pm 0.4 \times 10^{7}$
120	$9.0 \pm 0.2 \times 10^{4}$	$6.4 \pm 0.9 \times 10^{6}$	$6.2 \pm 0.9 \times 10^{7}$
150	$1.2 \pm 0.3 \times 10^{5}$	$6.9 \pm 0.2 \times 10^{6}$	$8.6 \pm 0.2 \times 10^{7}$

a. Mice were infected with 1.6×10^{4} bacteria intranasally.

Table 3. Lung infection following aerosol administration of MAC A5 and isogenic mutants 5G4 and 6H9.

M. avium strains	cfu per lung[a,b]	
	1 week	3 weeks
A5	$4 \pm 0.2 \times 10^{3c}$	$9.2 \pm 0.6 \times 10^{5c}$
5G4	$3.1 \pm 0.2 \times 10^{1c}$	$5.7 \pm 0.2 \times 10^{2c}$
6H9	$2.0 \pm 0.4 \times 10^{1c}$	$2.1 \pm 0.4 \times 10^{2c}$

a. The experiment was performed twice; the numbers represent the mean ± SD.
b. Mice were infected with 1.6×10^{4} bacteria intranasally.
c. $P < 0.05$ compared with the wild-type bacterium.

Mice infection

Infection of mice by the nasal route resulted in infection of the bronchiolar epithelium and dissemination. Table 2 shows the bacterial load in the lungs, spleen and liver after intranasal infection. Infection achieved a greater level in the lungs than in spleen and liver; however, it is clear that bacteria were capable of dissemination early in the infection. Figure 6 shows that, in *in vivo* model, *M. avium* is seen in the submucosa of the bronchioles at 15 days after infection. In subsequent experiments, the strain MAC A5 was used to infect mice in parallel to the isogenic strains 5G4 and 6H9. As shown in Table 3, while MAC A5 establishes lung infection, the biofilm-deficient mutants were significantly impaired in their ability to cause lung infection.

Discussion

Mycobacterium avium infection of the lung is usually seen in patients with chronic lung disease such as emphysema, bronchiectasis or cystic fibrosis (Inderlied *et al.*, 1993; Fujita *et al.*, 1999; Aksamit, 2002; Ebert and Olivier, 2002; Ebihara and Sasaki, 2002). *M. avium* can also be a cause of infection in elderly women and in individuals with deformities of the chest (Ebert and Olivier, 2002). More recently, cases have been described in people without any known predisposition, with the infection leading to secondary bronchiectasis (Prince *et al.*, 1989). The infection is many times chronic and treatment is of limited success because of the development of drug resistance (Griffith *et al.*, 1998; 2000). Patients infected with *M. avium* in the lung tend to respond to therapy initially but recurrence of infection shortly after the end of the course of treatment is common (Griffith *et al.*, 1998; 2000).

Histopathologically, *M. avium* infection of the lung is quite different from *Mycobacterium tuberculosis* infection. Peribronchiolar granulomas are the common finding, suggesting that the bacterium may cross the bronchiolar and bronchial mucosa (Kubo *et al.*, 1998). In this study, we showed that *M. avium* strains can infect and translocate across human bronchiolar cells *in vitro*. Interestingly, the

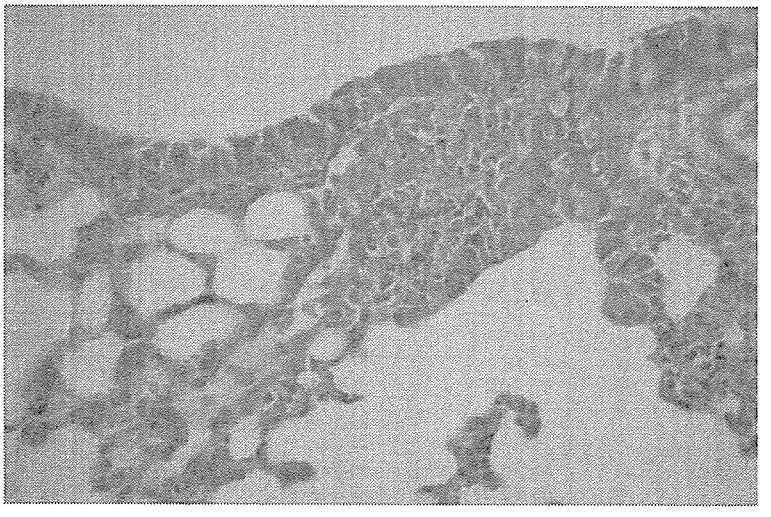

Fig. 6. Mice were infected intranasally with *M. avium* 104. Animals were harvested at the time points 2 weeks and 4 weeks. Bacterium is seen underneath the bronchial mucosa at 2 weeks after infection, demonstrating the route of infection.

infection of bronchial epithelial cells is more efficient after 24 h of contact. This observation suggests that either the bacterium upregulates invasion-related genes upon contact with the host cells, or still secreted proteins may have a role in the invasion. Subsequent experiments to address this question demonstrated that bacteria in contact with bronchiolar epithelial cells appear to develop the invasive phenotype, and the supernatant has no participation in the process.

Formation of biofilm is a common property of a number of bacterial pathogens. The Centers of Disease Control estimates that in approximately 50% of the human infections, biofilms play a role. Mycobacteria have been shown to form biofilm, and this characteristic has been investigated in *M. smegmatis* and *M. avium* (Recht and Kolter, 2001; Carter *et al.*, 2003). The possibility that clumping would influence the formation of biofilm/aggregates was ruled out by the preparation of the bacterial suspension. *M. avium* is capable of forming biofilm in urban PVC pipes, and it can easily be reproduced *in vitro* using PVC plates (Carter *et al.*, 2003; Primm *et al.*, 2004). The clinical course of *M. avium* lung infection is suggestive of the presence of biofilm, which would explain the chronic nature of the infection and poor response to treatment. In fact, recent studies demonstrate that *M. avium* biofilm is resistant to the action of antibiotics commonly used to treat the infection, such as clarithromycin, azithromycin and moxifloxacin (Carter *et al.*, 2004).

The role of biofilm on the infection of bronchiolar cells has been strengthened by the results of experiments using biofilm-deficient mutants of *M. avium*. Recently, glycopeptolipids have been associated with biofilm formation in both *M. avium* and *M. smegmatis* (Recht and Kolter, 2001; Carter *et al.*, 2003; Yamazaki *et al.*, 2006). The genetics of biofilm formation has been studied in *M. smegmatis*. The transposon mutagenesis of GPL gene cluster in *M. smegmatis* decreases the production of biofilm, and the inactivation of the *tmtp* genes significantly diminish the ability of the bacterium to form biofilm (Carter *et al.*, 2003). *M. avium* genes involved in GPL biosynthesis are associated with biofilm (Yamazaki *et al.*, 2006). Interestingly, the GPL cluster has been shown to differ between the strain 104 and strain A5 of *M. avium* (Krzywinska and Schorey, 2003), perhaps explaining the differences in the biofilm formation between these strains. Why biofilm mutants do not invade BEAS-2B cells like the wild-type bacterium is currently unknown. However, the inability to form biofilm could decrease the binding efficiency to the host cells or impact the regulation of invasion-related genes that are upregulated in the biofilm environment. The latter hypothesis appears more consistent with our results. In fact, recent observation with *Pseudomonas aeruginosa* proposes that regulatory genes for biofilm formation also influence the expression of the type III secretion system (Kuchma *et al.*, 2005). Therefore, it might be the case that genes regulating biofilm expression in *M. avium* are also involved in other aspects of virulence. Future studies will attempt to identify the genes upregulated under the biofilm conditions.

The results *in vitro* were confirmed by the observation in mice. The intranasal delivery of small inoculum ensured that most of the bacteria deposit on the bronchial and bronchiolar surface, and not in the alveolar space as observed in mice infected using aerosol chamber (Cooper *et al.*, 1998). The increase contact with the bronchiolar mucosa has as a consequence the development of peribronchiolar disease like in the great majority of humans with the infection (Kubo *et al.*, 1998). Whether biofilms are present on the mucosa in mice is currently unknown.

In many individuals, *M. avium* infection follows the development of pulmonary injury secondary to chronic obstructive disease. Work by Middleton *et al.* (2000), using tissue obtained from patients, demonstrated that *M. avium* was capable of binding to injured, unciliated epithelium but not to ciliated one. The authors also showed that fibronectin has a role in the binding to damaged epithelium with exposed extracellular matrix (Middleton *et al.*, 2000). In our model, fibronectin and possibly fibronectin attachment protein have a limited role on the binding and invasion of bronchial cells. It may be due to the absence of injury and extracellular matrix in our model. Nonetheless, the likelihood is that both models are relevant to the *in vivo* situation. In addition, the most recently described syndrome of chronic *M. avium* infection in patients without predisposing conditions may (Prince *et al.*, 1989) follow the model described in this study.

In summary, our study demonstrates a possible role for biofilm on the bronchiolar and bronchial infection by *M. avium*. The development of this model can add to our knowledge about the pathogenesis of *M. avium* infection and can also help in the development of more effective forms of therapy.

Experimental procedures

Mycobacteria strains

Mycobacterium avium A5, *M. avium* 104 and *M. avium* 101 were isolated from the blood of patients with AIDS. Isogenic mutants of the strain A5, clones 5G4, 6H9 and 9B5 with mutations on the genes homologous to *M. tuberculosis* strain H37Rv1565c, *suc*A and *pcd* were obtained by screening a transposon bank for deficiency in biofilm formation (Yamazaki *et al.*, 2006). Briefly, the transposon library was constructed by transforming the strain A5 with the plasmid pTN6JK-Kan, a plasmid containing a temperature-sensitive mycobacterial origin of replication, and the transposon Tn*5367* with a kanamycin-R cassette. After establishment of the bank, it was screened for impaired ability to form biofilm in PVC plates, as described (Carter *et al.*, 2003). Clones 5G4,

6H9 and 9B5 were among the selected. In all three clones, the transposon is inserted in the middle of the genes and complementation of the mutant strain with the functional gene is associated with recovery of the phenotype, which implies that the transposon did not disturb transcription of downstream genes. Bacteria were cultured on 7H10 agar plates or in 7H9 broth with oleic acid, albumin, glucose and catalase for 7 days at 37°C. The mutants were cultured in media supplemented with 400 μg ml^{-1} kanamycin. Complementation of the strains 5G4, 6H9 and 9B5 was carried out as previously described (Li *et al.*, 2005).

Assay of biofilm on PVC plate

Biofilm was established and evaluated as previously described (Carter *et al.*, 2003). Briefly, 1×10^8 bacteria in 200 ml of Hank's buffered salt solution (HBSS) were seeded in PVC 96-well microplates (Becton Deckinson). Following inoculation, plates were incubated at 30°C for up to 14 days. To measure the biofilm formation, supernatant was gently removed from each well, and 25 μl of a 1% crystal violet solution was added to each well (the dye stains bacterial cells but not the PVC material). The plates were incubated at room temperature for 15 min, rinsed vigorously four times with water, blotted on paper and scored for the presence of biofilm. The crystal violet was dissolved in 95% ethanol, and the A_{570} was determined, as previously described using a spectrophotometer (Carter *et al.*, 2003).

Invasion assay using BEAS-2B cells

The BEAS-2B cell, a human bronchial epithelial cell line, was purchased from the American Type Culture Collection (ATCC, Rockville, MD). The BEAS-2B cells were cultured in bronchial epithelial basal media supplemented with 52 μg ml^{-1} bovine pituitary extract, 0.5 mg ml^{-1} hydrocortisone, 0.5 ng ml^{-1} human recombinant epidermal growth factor, 0.5 μg ml^{-1} epinephrine, 10 μg ml^{-1} transferrin, 5 μg ml^{-1} insulin, 6.5 μg ml^{-1} retinoic acid and 65 μg ml^{-1} triiodothyronine (BEGM) (Cambrex Bio Science, Walkerville, MD). The BEAS-2B cells were cultured in T-75 or T-25 tissue flasks and were used between passages 3 and 10. Cells were cultured at 37°C in an atmosphere of 5% CO_2. For the invasion assay, BEAS-2B cells were seeded (1×10^5 cells per well) in a 24-well tissue culture plate (Coster, Corning, NY) and incubated until greater than 90% confluence was obtained (approximately 5 days).

To establish the inoculum, isolated bacterial colonies were obtained from 7H11 agar, added to 10 ml of HBSS, vortexed for 1 min and left to stand for an additional 30 min. The suspension was adjusted to MacFarland 1.0 [approximately 3×10^8 colony-forming units (cfu) ml^{-1}].

The invasion assay was performed as reported previously (Bermudez and Young, 1994; Sangari *et al.*, 2000). Briefly, before the assay, the culture medium of the monolayers was removed and replenished by warm culture medium. Monolayers were infected with 5×10^6 cfu bacteria and incubated at 37°C in a 5% CO_2 atmosphere for 2 h and 24 h. Cells were washed three times with HBSS, and treated with amikacin at a concentration of 200 μg ml^{-1} for 2 h. Amikacin, an aminoglycoside antibiotic, at the concentration used [approximately 20 times the minimum inhibitory concentration (MIC)], kills extracellular bacteria in 2 h, while intracellular bacteria remain viable (Bermudez and Young, 1994; Sangari *et al.*, 2000). The monolayers were washed three additional times with HBSS, and the viable intracellular bacteria were released by incubation with 0.5 ml of 1% Triton X-100 (Sigma) in sterile water for 15 min. The samples were harvested and vortex was agitated for 3 min to lyse cells. The numbers of viable bacteria were serially diluted in 0.1% Tween 80 and then plated onto 7H11 agar plates for quantification.

Effect of pre-incubation of M. avium *with bronchiolar cell on invasion*

The culture supernatant of BEAS-2B monolayer incubated with wild-type MAC A5 strain ($\sim 5 \times 10^6$ bacteria) for 24 h, as well as from uninfected monolayer, was collected. The recovered media were centrifuged at 3000 r.p.m. at 4°C, and the supernatants were separated from the pellet and kept at –70°C until required. Bacteria were also incubated with BEAS-2B monolayer for 24 h following treatment of the host cells with cytochalasin B, as described (Bermudez and Young, 1994), to prevent the uptake of bacteria. Extracellular bacteria were then recovered, separated from the supernatant, washed at 4°C and used to infect fresh monolayers.

Polarized cell layer on transwell

The BEAS-2B cells in BEGM were seeded at 0.2×10^5 cells per well on a transwell insert (Costar) containing 0.33 cm^2 porous filter membrane (3.0 μm pores). Polarized monolayers achieved confluence after 5 days at 37°C in 5% CO_2. Monolayers were incubated for 2 additional days until the transmonolayer electrical resistance reached the proper range (= 250 ohm), as measured with a Millicell-ESR apparatus (Millipore). In some experiments, transmonolayer electrical resistance was monitored as several time intervals after infection to assess damage to the monolayer. Dextran-FITC (Molecular Probes, Eugene, OR) was also used to monitor the integrity of the transwell, as previously described (Sangari *et al.*, 2000; Bermudez *et al.*, 2002). To determine bacterial translocation through both BEAS-2B monolayer, the 1×10^5 MAC were placed in the upper chamber and the supernatant of the lower chamber was obtained every 24 h. The supernatant was then replenished by fresh medium. The obtained supernatant was then plated onto 7H11 plates for quantification of the bacteria that crossed the cell layer.

Invasion assay in the presence of the anti-β1 integrin antibody

Invasion was carried out in the presence of anti-β1 integrin antibody, added to the BEAS-2B cells monolayer 2 h before the addition of bacteria. Antibody was maintained throughout the 2 h and 24 h invasion period. Several concentrations of anti-integrin antibody were examined, and the effect on internalization of wild-type bacterium was determined as described above. Non-specific antibody was used as control.

Electron microscopy

For electron microscopy, polarized monolayers on transwell inserts infected with bacteria were washed six times with HBSS

and fixed in cold (4°C) with 2.5% glutaraldehyde in 0.1 M phosphate buffer, pH 7.4, overnight. After washing in the same buffer, the transwell membranes were cut from the edge of the frame by using 18G needles and kept at 4°C. After washing with phosphate buffer, samples were post-fixed in cold 1% OsO_4 in the same buffer for 90 min. Samples were dehydrated in series of ethanol and embedded in epoxy resin, and ultra-thin sections (80 mm) were cut out of blocks and mounted on grids and stained with uranyl acetate and lead citrate before examination in a JEOL JEM-1230 transmission electron microscope. For scanning electron microscopy, the transwell membranes were fixed as described above, dehydrated in a critical point apparatus and examined with a JEOL JSM 6360 scanning electron microscope, after a Pt sputter coating.

Mice infection

To establish a model in which *M. avium* infection of the lung would resemble the patterns of infection observed in humans, we evaluated several techniques of mice infection by aerosol (data not shown). We concluded that the nasally infected mouse was the model that closely reproduces the human pathology. C57BL/6 mice were given $1.6 \pm 0.3 \times 10^4$ *M. avium* 101 strain intranasally. Mice were briefly anaesthetized with halothane and the bacterial suspension was delivered in the nostril by a 1 ml syringe with an 18-gauge needle. Five to 10 mice were used per time point. Mice were harvested at days 15, 30, 60, 90, 120 and 150. Spleen, liver and lung were weighed, then homogenized and plated as described (Kim *et al.*, 1998; Bermudez and Petrofsky, 1999). Lung tissue was also fixed with 1% formaldehyde, embedded in paraffin and stained using Ziehl-Nielssen stain, as previously reported (Kim *et al.*, 1998). In subsequent experiments using the strain A5 and isogenic mutants, infected mice were followed up to 4 weeks and harvested.

Statistical analysis

Analysis of variance (ANOVA) was used for the comparison among three or more groups. Student's *t*-test was used to compare means between the two groups. A P-value < 0.05 was considered statistically significant.

Acknowledgements

We thank Denny Weber for the careful preparation of the article. This work was partially supported by Grant #AI-43199 from the National Institute of Allergy and Infectious Diseases.

References

Abou-Zeid, C., Ratliff, T.L., Wiker, H.G., Harboe, M., Bennedsen, J., and Rook, G.A. (1988) Characterization of fibronectin-binding antigens released by *Mycobacterium tuberculosis* and *Mycobacterium bovis* BCG. *Infect Immun* **56:** 3046–3051.

Aksamit, T.R. (2002) *Mycobacterium avium* complex pulmonary disease in patients with pre-existing lung disease. *Clin Chest Med* **23:** 643–653.

Benson, C.A., and Ellner, J.J. (1993) *Mycobacterium avium* complex infection and AIDS: advances in theory and practice. *Clin Infect Dis* **17:** 7–20.

Bermudez, L.E., and Petrofsky, M. (1999) Host defense against *Mycobacterium avium* does not have an absolute requirement for major histocompatibility complex class I-restricted T cells. *Infect Immun* **67:** 3108–3111.

Bermudez, L.E., and Young, L.S. (1994) Factors affecting invasion of HT-29 and HEp-2 epithelial cells by organisms of the *Mycobacterium avium* complex. *Infect Immun* **62:** 2021–2026.

Bermudez, L.E., Sangari, F.J., Kolonoski, P., Petrofsky, M., and Goodman, J. (2002) The efficiency of the translocation of *Mycobacterium tuberculosis* across a bilayer of epithelial and endothelial cells as a model of the alveolar wall is a consequence of transport within mononuclear phagocytes and invasion of alveolar epithelial cells. *Infect Immun* **70:** 140–146.

Carter, G., Wu, M., Drummond, D.C., and Bermudez, L.E. (2003) Characterization of biofilm formation by clinical isolates of *Mycobacterium avium. J Med Microbiol* **52:** 747–752.

Carter, G., Young, L.S., and Bermudez, L.E. (2004) A subinhibitory concentration of clarithromycin inhibits *Mycobacterium avium* biofilm formation. *Antimicrob Agents Chemother* **48:** 4907–4910.

Cooper, A.M., Appelberg, R., and Orme, I.M. (1998) Immunopathogenesis of *Mycobacterium avium* infection. *Front Biosci* **3:** 141–148.

Dam, T., Danelishvili, L., Wu, M., and Bermudez, L.E. (2006) The fadD2 gene is required for efficient *Mycobacterium avium* invasion of mucosal epithelial cells. *J Infect Dis* (in press).

Ebert, D.L., and Olivier, K.N. (2002) Nontuberculous mycobacteria in the setting of cystic fibrosis. *Clin Chest Med* **23:** 655–663.

Ebihara, T., and Sasaki, H. (2002) Image in clinical medicine. Bronchiectasis with *Mycobacterium avium* complex infection. *N Engl J Med* **346:** 1372.

Fujita, J., Ohtsuki, Y., Suemitsu, I., Shigeto, E., Yamadori, I., Obayashi, Y., *et al.* (1999) Pathological and radiological changes in resected lung specimens in *Mycobacterium avium intracellulare* complex disease. *Eur Respir J* **13:** 535–540.

Griffith, D.E., Brown, B.A., Murphy, D.T., Girard, W.M., Couch, L., and Wallace, R.J., Jr (1998) Initial (6-month) results of three-times-weekly azithromycin in treatment regimens for *Mycobacterium avium* complex lung disease in human immunodeficiency virus-negative patients. *J Infect Dis* **178:** 121–126.

Griffith, D.E., Brown, B.A., Cegielski, P., Murphy, D.T., and Wallace, R.J., Jr (2000) Early results (at 6 months) with intermittent clarithromycin-including regimens for lung disease due to *Mycobacterium avium* complex. *Clin Infect Dis* **30:** 288–292.

Inderlied, C.B., Kemper, C.A., and Bermudez, L.E. (1993) The *Mycobacterium avium* complex. *Clin Microbiol Rev* **6:** 266–310.

Kim, S.Y., Goodman, J.R., Petrofsky, M., and Bermudez, L.E. (1998) *Mycobacterium avium* infection of gut mucosa in mice associated with late inflammatory response and intestinal cell necrosis. *J Med Microbiol* **47:** 725–731.

Krzywinska, E., and Schorey, J.S. (2003) Characterization of genetic differences between *Mycobacterium avium* subsp.

avium strains of diverse virulence with a focus on the glycopeptidolipid biosynthesis cluster. *Vet Microbiol* **91:** 249–264.

Kubo, K., Yamazaki, Y., Masubuchi, T., Takamizawa, A., Yamamoto, H., Koizumi, T., *et al.* (1998) Pulmonary infection with *Mycobacterium avium-intracellulare* leads to air trapping distal to the small airways. *Am J Respir Crit Care Med* **158:** 979–984.

Kuchma, S.L., Connolly, J.P., and O'Toole, G.A. (2005) A three-component regulatory system regulates biofilm maturation and type III secretion in *Pseudomonas aeruginosa*. *J Bacteriol* **187:** 1441–1454.

Li, Y., Miltner, E., Wu, M., Petrofsky, M., and Bermudez, L.E. (2005) A *Mycobacterium avium* PPE gene is associated with the ability of the bacterium to grow in macrophages and virulence in mice. *Cell Microbiol* **7:** 539–548.

Middleton, A.M., Chadwick, M.V., Nicholson, A.G., Dewar, A., Groger, R.K., Brown, E.J., and Wilson, R. (2000) The role of *Mycobacterium avium* complex fibronectin attachment protein in adherence to the human respiratory mucosa. *Mol Microbiol* **38:** 381–391.

Primm, T.P., Lucero, C.A., Falkinham, J.O., 3rd (2004) Health impacts of environmental mycobacteria. *Clin Microbiol Rev* **17:** 98–106.

Prince, D.S., Peterson, D.D., Steiner, R.M., Gottlieb, J.E., Scott, R., Israel, H.L., *et al.* (1989) Infection with *Mycobacterium avium* complex in patients without predisposing conditions. *N Engl J Med* **321:** 863–868.

Recht, J., and Kolter, R. (2001) Glycopeptidolipid acetylation affects sliding motility and biofilm formation in *Mycobacterium smegmatis*. *J Bacteriol* **183:** 5718–5724.

Reich, J.M., and Johnson, R.E. (1991) *Mycobacterium avium* complex pulmonary disease. Incidence, presentation, and response to therapy in a community setting. *Am Rev Respir Dis* **143:** 1381–1385.

Sangari, F.J., Goodman, J., and Bermudez, L.E. (2000) *Mycobacterium avium* enters intestinal epithelial cells through the apical membrane, but not by the basolateral surface, activates small GTPase Rho and, once within epithelial cells, expresses an invasive phenotype. *Cell Microbiol* **2:** 561–568.

Schorey, J.S., Holsti, M.A., Ratliff, T.L., Allen, P.M., and Brown, E.J. (1996) Characterization of the fibronectin-attachment protein of *Mycobacterium avium* reveals a fibronectin-binding motif conserved among mycobacteria. *Mol Microbiol* **21:** 321–329.

Yamazaki, Y., Danelishvili, L., Wu, M., MacNab, M., and Bermudez, L.E. (2006) *Mycobacterium avium* genes associated with the ability to form biofilm. *Appl Environ Microbiol* (in press).

APPLIED AND ENVIRONMENTAL MICROBIOLOGY, Jan. 2006, p. 819–825 Vol. 72, No. 1
0099-2240/06/$08.00+0 doi:10.1128/AEM.72.1.819–825.2006

Mycobacterium avium Genes Associated with the Ability To Form a Biofilm

Yoshitaka Yamazaki,[1] Lia Danelishvili,[1] Martin Wu,[1] Molly MacNab,[1] and Luiz E. Bermudez[1,2]*

Department of Biomedical Sciences, College of Veterinary Medicine,[1] and Department of Microbiology, College of Science,[2] Oregon State University, Corvallis, Oregon 97331

Received 6 September 2005/Accepted 24 October 2005

***Mycobacterium avium* is widely distributed in the environment, and it is chiefly found in water and soil. *M. avium*, as well as *Mycobacterium smegmatis*, has been recognized to produce a biofilm or biofilm-like structure. We screened an *M. avium* green fluorescent protein (GFP) promoter library in *M. smegmatis* for genes involved in biofilm formation on polyvinyl chloride (PVC) plates. Clones associated with increased GFP expression ≥2.0-fold over the baseline were sequenced. Seventeen genes, most encoding proteins of the tricarboxylic acid (TCA) cycle and GDP-mannose and fatty acid biosynthesis, were identified. Their regulation in *M. avium* was confirmed by examining the expression of a set of genes by real-time PCR after incubation on PVC plates. In addition, screening of 2,000 clones of a transposon mutant bank constructed using *M. avium* strain A5, a mycobacterial strain with the ability to produce large amounts of biofilm, revealed four mutants with an impaired ability to form biofilm. Genes interrupted by transposons were homologues of *M. tuberculosis* 6-oxodehydrogenase (*sucA*), enzymes of the TCA cycle, protein synthetase (*pstB*), enzymes of glycopeptidolipid (GPL) synthesis, and Rv1565c (a hypothetical membrane protein). In conclusion, it appears that GPL biosynthesis, including the GDP-mannose biosynthesis pathway, is the most important pathway involved in the production of *M. avium* biofilm.**

Mycobacterium avium complex is widely distributed in the environment, such as in water and soil, and is a chief component of many natural aquatic biofilms (8). *M. avium* is also known to cause chronic pulmonary infection in patients with predisposing lung disease, such as previous tuberculosis and chronic obstructive pulmonary disease (28). Urban water systems contain organisms of the *M. avium* complex in biofilm or a biofilm-like structure, and individuals can potentially be exposed to the bacterium, either by inhalation of aerosol particles or ingestion of contaminated water. Studies have established an association between *M. avium* in urban water and the development of disseminated disease in individuals with AIDS (36).

Mycobacterium smegmatis, as well as *M. avium*, has been shown to produce a biofilm or a biofilm-like structure (6, 19). The outermost layers of the *M. smegmatis* and *M. avium* cell walls contain glycopeptidolipid (GPL), whereas the outermost layer of *M. tuberculosis* is made of phenolic glycolipids, dimycocerosate, and lipo-oligosaccharides (24). Recent studies suggest that the *M. smegmatis* biofilm is associated with a GPL present on the cell wall, and indirect evidence indicates a similar role in *M. avium* (6). Aspects of biofilm formation have begun to be examined with *M. smegmatis*. Transposon inactivation of the GPL gene clusters in *M. smegmatis* decreased the production of biofilm, and the deletion of the genes *tmtp* and *mps* revealed their involvement in biofilm formation upon seeding of the bacterium on polyvinyl chloride (PVC) plates (19, 26). The *tmtp* gene is highly conserved between *M. smegmatis* and *M. avium*, with both organisms having genes encoding one small (*tmtpA*) and two large (*tmtpB* and *tmtpC*) putative transmembrane transport proteins in the same operon. The proposed function involves the transport of the precursor of GPL from the inner membrane. The *mps* genes are identified as *pstA*, *-B*, and *-C*, constituting the GPL gene clusters in *M. avium* (GenBank accession no. AF143772). The peptide synthetase (*mps*, Mps protein) has a role in the initial step of GPL synthesis, i.e., in the assembly of the lipopeptide core and acceptor of acyl-Phe, which is modified by sequential addition of threonine, alanine, and alaninol (4). This lipopeptide core may subsequently be glycosylated with rhamnose and 6-deoxytalose, resulting in the nonspecific GPL (nsGPL). The acetyltransferase (*atf1*) acetylates on 6-deoxytalose in the cell wall, and the putative *tmtpC* (Tmtpc) protein transports it to the outermost layer of the cell wall (4, 19, 26). However, the roles of GPLs in biofilm formation are still not well defined.

The genetic determinant of biofilm formation in *M. avium* has not been clearly identified. It was reported that *M. avium* A5 produced increased amounts of biofilm compared with the *M. avium* 101, *M. avium* 104, and *M. avium* 109 strains (6). Furthermore, *M. avium* strains produced more biofilm when inoculated in water than in 7H9 broth on a PVC surface. During biofilm formation, microorganisms rarely come into contact with a clean surface and normally colonize a surface that has been modified following the absorption of molecules from the environment, such as water and proteins, etc. The *M. avium* 101 and 104 strains belong to serotype 1, while *M. avium* A5 and strain 109 belong to serotype 4. Krzywinska and Schorey (17) described the genomic differences, especially in GPL gene clusters, between *M. avium* 104 (the strain from which the

* Corresponding author. Mailing address: Department of Biomedical Sciences, College of Veterinary Medicine, Oregon State University, 105 Magruder Hall, Corvallis, OR 97331. Phone: (541) 737-6538. Fax: (541) 737-2730. E-mail: luiz.bermudez@oregonstate.edu.

TABLE 1. Plasmids and strains used in this study

Plasmid vector	Relevant description	Reference
PUC18	ColE1 replicon, *ampR*	36
pCG79	Derivative of pCG 76, Km^r	13
pTNGJC	Transposon Tn*5367*	This study
GFP expression vector pEMC1	*M. avium* promoter library	8
Complemented construct (pMV261-AprII)	Derivative of pMV261, *hsp60* promoter, Apr^r	This study

genome sequence is available) and *M. avium* A5. Those authors identified that the GPL was highly conserved upstream of the GPL clusters methyl transferase B (*mtf* B), glycosyl transferase A (*gtf* A), rhamnosyl transferase A (*rtf* A), *mtf* C, *mtf* D, and dehydrogenase A (*dhg* A). But downstream of these gene clusters, the GPL is quite different between *M. avium* 104 and *M. avium* A5. In addition, it was shown that *M. avium* A5 has the GDP-D-mannose dehydratase *mdht* gene (GenBank accession no. AAD20373) and the GDP-6-deoxy-4-keto-D-mannose 3-5-epimerase-4-reductase *mer* gene (AAD20374) (17). These two enzymes catalyze the transformation of GDP-mannose to GDP-fucose (34). Since GDP-fucose is an important substrate for the GPL, especially for serovar-specific GPL, it is supposed to reflect the different means of biofilm formation between the *M. avium* 104 and *M. avium* A5 strains.

In this study, we used two strategies, the screening of a transposon mutant library and of a green fluorescent protein (GFP) promoter library to identify *M. avium* genes associated with biofilm formation on a solid surface that is encountered in water pipes.

MATERIALS AND METHODS

Mycobacterial strains and plasmids. *M. avium* A5 (2) and *M. avium* 104 are virulent strains, isolated from blood of patients with AIDS. *Mycobacterium smegmatis* mc^2155 was kindly provided by William Jacobs, Jr. (Albert Einstein School of Medicine) (32). They were cultured in either Middlebrook 7H11 agar or 7H9 broth containing 10% oleic acid, albumin, dextrose, and catalase, while *M. smegmatis* and *M. avium* mutant clones were plated onto 7H11 Middlebrook agar containing 50 μg/ml or 400 μg/ml of kanamycin, respectively.

Escherichia coli strain DH5α (Stratagene, La Jolla, CA) was used as the host for plasmid construction. GFP-mut2 genes were generated by PCR from the pKEN plasmid, obtained from Rafael Valdivia and Stanley Falkow, Stanford University. GFP-mut2 genes were cloned into the promoterless reporter plasmid pMV261 (9). Temperature-sensitive plasmid pTNGJC was constructed based on the pUC18 vector, as described previously (18).

Briefly, the transposon Tn*5367* was cut from pYUB285 and cloned in the EcoRI and HindIII restriction sites, making the plasmid pUC18-Tn5367 (Table 1). The transposon contains the kanamycin-resistant gene as a cassette. The temperature-sensitive mycobacterial origin of replication was removed from pCG79 (provided by B. Gicquel, Institute Pasteur, Paris, France) and inserted in pUC19-Tn5367, using the HindIII restriction site, to create pTNGJC. Transformation with pTNGJC in *M. avium* A5 was carried out according to protocol described previously (12).

Screening of the *M. avium* GFP promoter library. The *M. avium* GFP promoter library was constructed in *M. smegmatis* as previously described (9) and stored in pools of five in 96-well plates containing Middlebrook 7H9 broth with 50% glycerol at −70°C. Bacterial pools containing 5×10^7 bacteria were suspended in 200 μl of 7H9 broth and placed into 96-well tissue culture plates (Corning Inc., NY) at 37°C for 3 days. Then 100-μl aliquots of bacteria from each well were transferred to 96-well PVC plates (Becton Dickinson Labware, Franklin Lakes, NJ). The PVC plates were kept at room temperature for 5 days and assayed for the expression of GFP daily (CytoFluor II; subsidiary of Millipore Corp, MA). We were interested in gene up-regulation that precedes the formation of a biofilm. The pools with a ratio of the level of GFP at day 5 to that of GFP at day 1 of over 2.0 were subsequently diluted and plated onto 7H11 agar with 50 μg/ml kanamycin (Km) to obtain isolated clones (9). The experiment was then repeated, with individual isolates, and wells containing clones associated with increased GFP expression greater than 3.0-fold over the baseline were sequenced at the Central Service Laboratory, Oregon State University, using the GFP primer 5′-TTGTGCCCATTAACATCACCA-3′. Database search and sequence comparisons were performed using the BLAST network service at the National Center for Biotechnology Information (NCBI).

Construction of the *M. avium* A5 transposon library. *M. avium* A5 competent cells were washed with 10% glycerol three times at 4°C and 3,000 rpm and diluted in 1 ml 10% glycerol. Bacteria were submitted to electroporation using a Gene Pulser Xcell (Bio-Rad, CA) and plated on 7H11 agar with 400 μg/ml of kanamycin (9). A clone containing the plasmid pTNGJC-KAN was grown at 30°C for 3 weeks in 7H9 broth in the presence of 200 μg/ml of kanamycin. After the number of bacteria in suspension reached approximately 1×10^9 CFU, the culture was placed at 41°C for 3 days. Because pTNGJC-KAN contains a temperature-sensitive Myc origin of replication, the shift in temperature eliminated the plasmid, and all surviving kanamycin-resistant cells necessarily contained pTNGJC-KAN in the bacterial chromosome (18). The suspension was then diluted and plated onto 7H11 agar with kanamycin at 37°C. Colonies were harvested and screened by PCR for the presence of the kanamycin gene (Table 1). Primers for the Km gene were 5′-TGTTCAACAGGCCAGCCA-3′ (forward) and 5′-TAATGTCGGGCAATCAGGTG-3′ (reverse). Twenty colonies were selected and tested for the presence of the transposon-Km gene. All 20 contained the transposon.

Selection of clones deficient in biofilm formation. Biofilm (or biofilm-like) formation was determined as previously described (6). Briefly, 1×10^8 bacteria in 200 μl of Hanks' buffered salt solution (HBSS) were seeded on PVC 96-well microplates. Plates were incubated at 37°C for up to 14 days. To measure the biofilm formation, the supernatant was removed gently from each well, and 25 μl of a 2% crystal violet solution was added to each well (the dye stains bacterial cells but not the PVC material). The plates were incubated at room temperature for 15 min and rinsed three times with HBSS. The crystal violet was dissolved in 95% ethanol, and biofilm formation was analyzed at 570 nm, as previously reported (6, 26). Two thousand mutants were screened. The experiments were repeated at least five times.

Identification of the transposon-inactivated gene. The genes inactivated were identified by using a nonspecific, nested suppression PCR (34). The primer used was 5′-CCATCATCGGAAGACCTC-3′. PCR cycling was as follows: 35 cycles of 94°C for 30 s, 50°C for 1 min, and 72°C for 4 min. Prior to the first cycle, a temperature of 94°C was held for 5 min, and at the end of the last cycle, a temperature of 72°C was maintained for 7 min. The primer used for the second PCR was 6 nucleotides (GACCCC) longer at the 3′ end. The PCR cycling was the same as the first PCR, except the annealing cycle was for 30 s at 56°C using *Pfu* DNA polymerase (Stratagene). The PCR products were run in 1% agarose gel, and each PCR band that appeared on the gel was cut and extracted using a gel extraction kit (QIAGEN). The PCR amplifications were cloned into the pCR2.0 TOPO vector (Invitrogen, Carlsbad, CA) and submitted for sequencing (18).

Complementation of the mutants. The sequences of the isogenic mutants of 5G4 (*MA1565c*), 6H9 (*sucA*), and 9B5 (*pcd*) were obtained using the *M. avium* 104 genome BLAST network service of the NCBI. The primers for selected genes were 5G4 forward (5′-GAG AAT TCG CGG GTT TTC GGT AAA TTA GC-3′), 5G4 reverse ('-GTA AGC TTT TTC GAG GCG GCA GAG CCG AT-3′ [2,232 bp]), 6H9 forward (5′-GAG AAT TCA TGT ACC GCA AGT TCC GCG AC-3′), 6H9 reverse (5′-GTA AGC TTT CGG GCA GCT CCA GGC CGA AT-3′ [3,573 bp]), 9B5 forward (5′-GAG AAT TCG AGC ACG CGA TAA CCC AAG CA-3′), and 9B5 reverse 5′-GTA AGC TTA ATC GCG TCG TCC AGC CGG TC-3′ [1,091 bp]). The genes were amplified by PCR, and then the product was digested with both EcoRI and HindIII restriction enzymes. The genes were inserted into EcoRI and HindIII restriction sites of the pMV261-AprII plasmid. The plasmid was transformed into *E. coli* competent cells (DH5a-T1 chemical competent cell [Invitrogen]) for replication. The plasmid

TABLE 2. *M. avium* genes identified as up-regulated upon incubation on PVC plates using the GFP promoter library

Clone(s)	Gene	Protein	Homologue of *M. tuberculosis* H37Rv or CDC1551	Fold increase in GFP expression
4A11	*gtf*	Glycosyltransferase	MT0564	3.6
4D7, 4H5, 5E12, 12B7, 1C9	*guaB2*	IMP dehydrogenase	Rv3411	3.8
4H11	*ccsA*	Cytochrome *c*-type biogenesis protein	Rv0529	3.2
10H6	*accD2*	Acetyl/propionyl-CoA carboxylase (β subunit)	Rv0974	4.0
19H7	*pks10*	Polyketide synthase family	Rv1660	3.5
22A2, 22H3	*pmmB*	Mannose-1-phosphatase	Rv3308	3.8
22H5	*accA2*	Acetyl/propionyl-CoA carboxylase (α subunit)	Rv0973	3.4
22B8	*ltp3*	Lipid carrier protein or keto acyl-CoA thiolase	Rv3523	3.9
3A12		Integral membrane protein[a]	Rv0359	4.1
20B5		Acid phosphatase[a]	Rv3310	3.2
5B10		Oxidoreductase[a]	Rv3526	3.8
22H7		Integral membrane transport protein[a]	Rv1258c	3.7

[a] Probable hypothetical protein.

was then purified using a plasmid extraction kit (Stratagene). Plasmids containing the functional genes were electroporated into 5G4, 6H9, and 9B5 competent cells, as described above. The bacteria were then plated onto 7H11 agar containing 400 μg/ml apramycin (Apr). The PCR production was cloned into the pMV261-AprII plasmid containing the *hsp60* promoter upstream of the genes and an Apr-resistant gene to create pMV261-5G4, pMV261-6H9, and pMV261-9B5. To confirm transformation, the Apr gene was identified by PCR application; the primers for the Apr gene were 5′-GCATCGCATTCTTCGCATCC-3′ (forward) and 5′-GGCCCACTTGGACTGATCGA-3′ (reverse).

RNA extraction and RT. *M. avium* strains were grown in 7H9 broth with 10% oleic acid, albumin, dextrose, and catalase for 5 days (1×10^9/ml) and then pelleted at 3,000 rpm for 15 min at room temperature, resuspended in HBSS, and inoculated on PVC plates for 7 days. Bacteria grown in 7H9 broth at 37°C were used as the control. The bacterial pellets recovered from PVC plates were submitted to RNA extraction. Total RNA was isolated by rapid mechanical cell lysis in a guanidine thiocyanate-based buffer (Trisol) (Invitrogen) in the following manner. The supernatant was removed and added to a 2-ml tube containing the Heavy Phase Lock Gel (Eppendorf, Westbury, NY) and 300 μl chloroform-isoamyl alcohol (24:1). Inverting rapidly, aliquots were centrifuged for 10 min at 4°C, and the aqueous layer was collected and precipitated with isopropanol. Then the pellet was washed with 75% ethanol and dried at room temperature. RNA samples were treated with DNase I (Clontech, Palo Alto, CA) and incubated for 30 min at 30°C. The RNA quantity was determined on 1% denaturing agarose gel, the concentration was calculated, and the quality was determined spectrophotometrically by determining absorption (optical density at 260 or 280 nm). Total RNA was reverse transcribed, and the resulting cDNA was amplified by the SuperScript First Strand synthesis system for reverse transcription (RT)-PCR (Invitrogen) in the following manner. Briefly, total RNA (3 μg) was incubated with 1 μl of a 10 mM concentration of a deoxynucleoside triphosphate mix, 1 μl of random hexamers, and diethyl pyrocarbonate-treated water at 65°C for 5 min and then mixed with 2 μl of 10× RT buffer, 4 μl 25 mM $MgCl_2$, 2 μl 0.1 M dithiothreitol, and 1 μl RNase OUT recombinant RNase inhibitor at 42°C for 2 min. One microliter of SuperScript II reverse transcriptase was added to each tube, and the tube was incubated at 42°C for 50 min. The reaction was terminated at 70°C for 15 min, and the tube was chilled on ice.

Quantitative real-time RT-PCR assay. Quantitative fluorogenic amplification of cDNA was performed using the iCycler real-time detection system (Bio-Rad) and SYBR green technology (Bio-Rad), according to the method previously described (9). The relative abundances from standard curves were determined from a serially diluted standard pool of cDNAs and normalized to the 16S rRNA mRNA levels. The following primers were designed based on a BLAST search of the NCBI database: *guaB2* (1,009 bp; forward, 5′-TCA CCT GCC GCC CCG

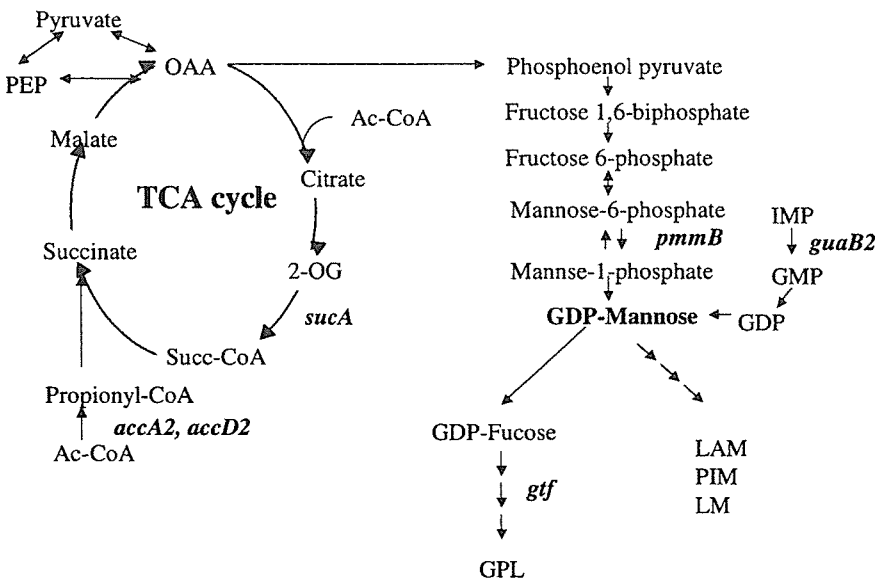

FIG. 1. Genes of biofilm formation associated with the TCA cycle and GDP-mannose and glycopeptidolipid biosynthesis. The TCA cycle provides phosphoenolpyruvate, converted from oxaloacetate (OAA). The *pmmB2* and *guaB2* genes encode the enzymes to accelerate the biosynthesis of GDP-mannose. The *gtf* gene encodes the enzyme to biosynthesize GPL. Ac, acetyl; PEP, phosphoenolpyruvate; 2-OG, alpha-ketoglutarate; LAM, lipoarabinomannan; PIM, phosphatidylinositol mannoside; LM, lipomannan.

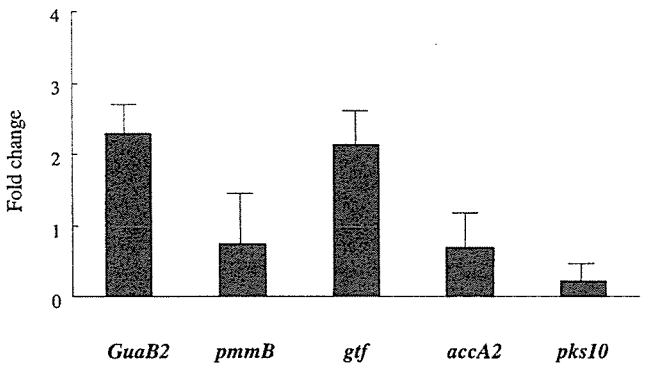

FIG. 2. Changes in mRNA expression (n-fold) in *M. avium* A5 using real-time PCR. The expression of *guaB2*, *gtf*, *pmmbB*, *accA2*, and *pks10* in *M. avium* A5. The expression of *guaB* and *gtf* was greater in *M. avium* A5 than in 104, while the expression of *pks* mRNA in *M. avium* A5 was lower than in *M. avium* 104. Values are means ± standard deviations (n = 3). The levels of expression of *pmmB* and *accA2* were comparable in both strains. A P of <0.05 was considered significant for the expression of all genes.

ACA ACA CGC TGC CCC-3′; reverse, GGC ACC CGG CCC TCG ATG CCC TCG GGC ACC-3′), *pmmB* (787 bp; forward, 5′-TCC CGA CCC CCG CAC GGC CGC-3′; reverse, 5′-GTC CAC ATC GGC GGC CAG GGT-3′), *gtf* (374 bp; forward, 5′-ATG GAC GGC GCC GAC CTG CCC-3′; reverse, 5′-AGG ATC GCG GTG ATG CTG CCC-3′), *accA2* (1,157 bp; forward, 5′-CGG TGG ATG CGG TGC GCG CGA TGG GCT-3′; reverse, 5′-GTT CCG CCA GCC GCT GGG GAT-3′), *pks10* (106 bp; forward, 5′-ATG AGC GTC ATC GCC GGC GTG-3′; reverse, 5′-TCA GTG CCA ACG CAA CAA CAC-3′), and 16S rRNA (934 bp; forward, CGA ACG GGT GAG TAA CAC G-3′; reverse, 5′-TGC ACA CAG GCC ACA AGG GA-3′). The cDNA was denatured for 5 min at 95°C, followed by 30 cycles of amplification. Each cycle consisted of denaturation at 95°C for 30 s, annealing at 60°C for 30 s, and primer extension at 72°C for 2 min. The threshold cycle (Ct), which is defined as the fractional cycle number at which the fluorescence reaches 10 times the standard deviation of the baseline, was quantitated as described in User Bulletin no. 2 for the ABI PRISM 7700 sequence detection system. Changes in (Δ) gene expression (n-fold) were calculated as follows: $\Delta Ct_{target} = Ct_{M.\ avium\ A5\ mRNA} - Ct_{16S\ rRNA}$; $\Delta Ct_{control} = Ct_{M.\ avium\ 104\ mRNA} - Ct_{16S\ rRNA}$; and $\Delta(\Delta Ct) = \Delta Ct_{target} - \Delta Ct_{control}$; change ($n$-fold) = $2^{-\Delta(\Delta Ct)}$.

Statistical analysis. Analysis of variance was used for the comparisons among three or more groups. Student's t test was used to compare means between the two groups. The P values that were <0.05 were considered statistically significant.

RESULTS

Biofilm-associated promoters identified using a GFP promoter library. To identify *M. avium* genes regulated upon the formation of a biofilm or biofilm-like structure on PVC, an *M. avium* promoter library containing 10,000 clones of *M. smegmatis* was screened. Because we were interested in genes expressed during the initial phase of biofilm formation, GFP expression was monitored during the first 5 days of *M. avium* exposure to PVC. Twelve clones were identified with increased expression of GFP. Sequencing of the 12 genes showed that *guaB2* (IMP dehydrogenase), *AccA2* and *AccD2* (alpha and beta subunits of acetyl/propionyl coenzyme A [CoA] carboxylase, respectively), *pks10* (polyketide synthase family), *pmmB* (mannose-1-phosphatase), *Itp3* (lipid carrier protein or keto acyl-CoA thiolase LTP3), *ccsA* (cytochrome *c*-type biogenesis protein), and *gtf* (glycosyl transferase, a homologue of *M. tuberculosis* CDC1551) were up-regulated. Four genes out of the 12 encode hypothetical proteins (Table 2). The *AccA2* and *AccD2* genes encode enzymes which are part of the TCA cycle (Fig. 1). The *guaB2* and *gtf* genes take part in the biosynthesis of GDP-mannose and GPLs, respectively, as shown in Fig. 1.

Detection of *M. avium* mRNA expression using real-time PCR. To confirm the findings obtained by screening the GFP promoter library, five genes were selected and real-time PCR was performed using *M. avium* strains seeded on PVC plates. The genes *guaB2* and *gtf* were chosen because they represent different pathways, while *pks10* was selected due to the importance of polyketides in mycobacteria. The *M. avium* 104 and *M. avium* A5 strain mRNAs were obtained from bacteria growing on PVC plates for 5 days. All five genes showed a significant increase ($P < 0.05$ using Student's t test) of expression upon biofilm formation, and the levels of expression of two genes were comparable between the strains A5 and 104, although the level of expression sometimes varied. The levels of expression of *guaB2* and *gtf* in the *M. avium* A5 strain were increased, respectively, 2.28 ± 0.37- and 2.12 ± 0.46-fold above the levels of expression of similar genes in the *M. avium* strain, while expression of the *pks10* gene of *M. avium* A5 decreased by 0.21 ± 0.25-fold compared with that of *M. avium* strain 104 (Fig. 2). These data confirmed the relevance of the promoter assay.

***M. avium* A5 transposon mutants attenuated on biofilm formation.** As shown in Table 3, the screening of the transposon library led to the identification of five clones with an impaired ability to form biofilm. The possibility that the mutants would bind more to the crystal violet was ruled out by preliminary analysis with a similar number of mutant and wild-type bacteria stained with crystal violet. Four sequences were obtained out of the five mutants. The 2F1 and 6H9 mutants have the transposon inserted in the gene homologous to *M. tuberculosis* H37Rv *sucA* (Rv1248c), which encodes 2-oxoglutarate dehydrogenase. The 5G4 mutant had inactivation of a gene encoding a hypothetical membrane protein (Rv1565c), while the 9B5 mutant had the transposon interrupting a *pcd* (Rv3293) homologue of piperideine-6-carboxylic acid dehydrogenase (P6CDH). The 4B2 mutant had inactivation of a gene homol-

TABLE 3. *M. avium* genes identified using the transposon mutant system

Clone(s)	Gene(s)	Protein	Homologue of *M. tuberculosis* H37Rv or CDC1551
4B2	*nrp* (*pstB*)[a]	Protein synthetase	Rv0101
5G4		Hypothetical membrane protein	Rv1565c
2F1, 6H9	*sucA*	2-Oxoglutarate dehydrogenase	Rv1248
9B5	*pcd*	Piperideine-6-carboxylic acid dehydrogenase	Rv3293

[a] Homologue of the *M. avium* 2151 genome (GenBank accession no. AF143772).

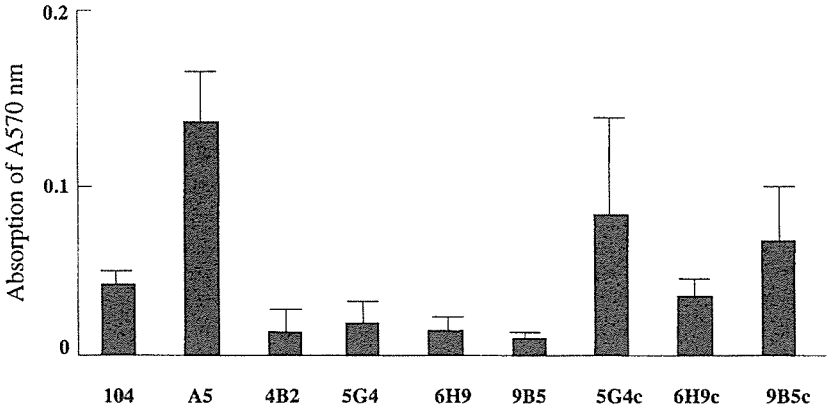

FIG. 3. Biofilm formation by the *M. avium* wild-type strain, transposon mutants, and strains with complementations of the inactivated genes. The bacterial strains (6×10^8 CFU/ml) were inoculated on PVC 96-well plates with HBSS for 14 days. The biofilm was evaluated using crystal violet stain as described in Materials and Methods. Values are means ± standard deviations. The A_{570} readings from three experiments are shown. 5G4, 6H9, and 9B5 were the transposon mutants of *M. avium* A5 strain. 5G4c, 6H9c, and 9B5c were the complemented strains of transposon mutants. A P of <0.005 was used for the comparisons between 4B2, 5G4, 6H9, 9B5, and 104 or A5. A P of >0.005 was used for the comparisons between 5G4 and 5G4c, 6H9 and 6H9c, and 9B5 and 9B5c.

ogous to the *pstB* gene of the *M. avium* 2151 genome (GenBank accession no. AF143772).

Biofilm formation by the wild type, mutants, and complemented strains. The ability to form biofilm was evaluated comparatively among the wild-type, mutant, and complemented strains. *M. avium* 104 and *M. avium* A5 had a spectrophotometer reading of 0.041 ± 0.001 and 0.136 ± 0.031. Biofilm formation of mutants 5G4 (0.019 ± 0.012), 6H9 (0.014 ± 0.009), and 9B5 (0.010 ± 0.002) was significantly impaired compared with that of *M. avium* A5. The biofilm formation of complemented strains 5G4c (0.082 ± 0.064), 6H9c (0.034 ± 0.009), and 9B5c (0.067 ± 0.041) was significantly increased compared with that of the 5G4, 6H9, and 9B5 mutants (Fig. 3), although no complete complementation was achieved.

Colony morphology of *M. avium* A5 strain and mutants and between mutant and complemented strain. The colony morphology of *M. avium* A5 appears like a white dome on 7H11 agar for 30 days (Fig. 4). On the other hand, the colonies of the depleted transposon mutants 5G4, 6H9, and 9B5 were white, flat, and round with a central small dome on 7H11 agar with Km at 400 μg/ml. The complemented transposon mutants of 5G4, 6H9, and 9B5 were all white and formed a dome on 7H11 agar, with Km at 400 μg/ml and Apr at 400 μg/ml, which were almost the same shape as the *M. avium* A5 strain. All mutant strains grew in agar in a fashion similar to that of the wild-type A5 strain (data not shown) at 37°C.

DISCUSSION

M. avium is an environmental bacterium that can infect humans. *M. avium* is known to form biofilm or biofilm-like structures, and it is commonly recovered from sauna walls, swimming pools, and urban PVC water pipes. The ability to form biofilm has been associated with chronic bacterial infection. Persistent *M. avium* infection is frequently seen in individuals with chronic lung pathology, such as emphysema and cystic fibrosis. Since it is plausible that the ability to establish a biofilm can be associated with the difficulty to eliminate the infection, we attempted, as the first stage, to identify bacterial genes involved in biofilm formation. We screened an *M. avium* GFP promoter library of *M. smegmatis* and an *M. avium* transposon library. The use of an *M. avium* library with *M. smegmatis* is a very effective and rapid strategy that can have the results confirmed by investigating the transcription of identified genes in *M. avium* (9).

The GFP assay revealed several genes, up-regulated concomitantly with the formation of the biofilm. Two of the genes (*AccA2* and *AccD2*) were members of the TCA cycle and have homology to the alpha and beta subunits of acetyl/propionyl-

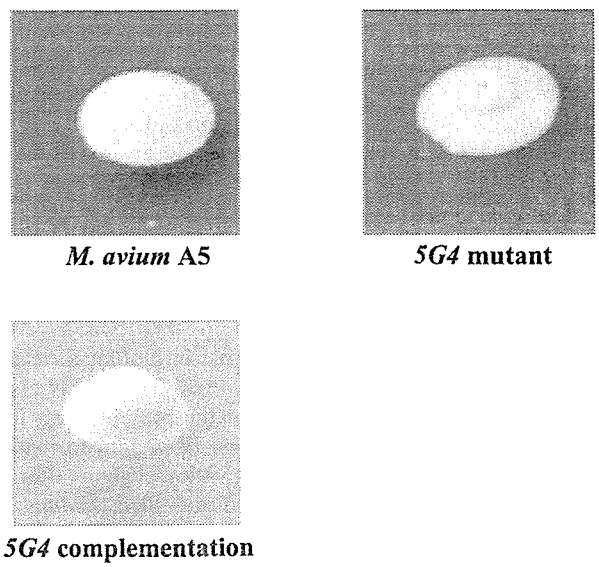

FIG. 4. Colony morphologies of *M. avium* A5, its transposon mutants, and its complemented strains. *M. avium* A5 was cultured and observed for 30 days on 7H11 agar. The transposon mutant, 5G4, was grown on 7H11 with 400 μg/ml of kanamycin, and its complementation, 5G4c, was grown on 7H11 with 400 μg/ml of kanamycin and 400 μg/ml of apramycin.

CoA carboxylase, respectively. Three genes (*guaB2*, *pmmB*, and *gtf*) are associated with GDP-mannose and GPL biosynthesis. The *Itp3* and *pks10* genes encode proteins that participate in fatty acid biosynthesis, while the other identified genes encode hypothetical proteins.

Biofilm formation occurs by phases in which the levels of gene regulation may differ. In our screen, we were interested in genes up-regulated during the establishment of the biofilm and not later phases. Synthesis of GPL, therefore, must be important for the adherence and initial establishment of biofilms.

In the synthesis of GPL, phosphoenolpyruvate is synthesized from oxaloacetate in the TCA cycle (22, 35). The pathway leads to GDP-mannose through fructose 1,6-biphosphate, fructose 6-phosphate, mannose-6-phosphate, and mannose-1-phosphate. The GDP-mannose is provided by two different biosynthetic pathways (Fig. 1), which suggests the importance of the pathway. The gene *pmmB*, which was identified by a GFP promoter library in the present study, is homologous to mannose-1-phosphatase. In an alternate pathway for GPL synthesis, the GDP may be synthesized. GDP is a product of the conversion of GMP and IMP, and the enzyme IMP dehydrogenase (*guaB2*) converts IMP into GMP. Considering mRNA expression upon biofilm formation, *guaB2* expression was greater than that of *pmmB*, perhaps implying increased importance of the pathway under the conditions used. However, only by creating a null mutation on the genes can this hypothesis be addressed. The reason the synthesis of IMP appears to be of more significance than the synthesis of mannose-6-phosphate for biofilm formation is presently unknown.

GDP-fucose synthetase converts GDP-mannose to GDP-fucose. Fucose is found widely distributed in complex carbohydrates as a component of glycoconjugates, such as glycoproteins and glycolipids, in a wide variety of bacteria (15, 20). Fucose is added to glycoconjugates by specific transferases that utilize GDP-fucose as the sugar donor. In gram-negative bacteria, fucose is present as a component of the capsular polysaccharides and lipopolysaccharides which function in antigenic determination and participate in biofilm formation. On the other hand, GDP-mannose is the precursor of phosphatidylinositol and phosphatidylinositol mannosides in *M. tuberculosis*. GDP-mannose also provides the lipid anchor of two lipoglycans, lipomannan and lipoarabinomannan, the latter being an important modulator of the immune response in the course of tuberculosis and leprosy (7, 23), as well as a key ligand in the interactions between *M. tuberculosis* and phagocytic cells (13, 30). However, the roles of phosphatidylinositol mannosides and lipoarabinomannan in *M. avium* have not been extensively studied, and their role in biofilm formation could be novel.

The genes which were identified in the present study have shed light on the metabolic regulation of biofilm formation. Martinez et al. (19) reported the inactivation of genes after use of the mariner transposon system and identified the *mps* and *tmtpC* genes as being involved in biofilm formation. The *mps* is homologue of a peptide synthetase (GenBank MAC 104 genome; *pstA*, *pstB*, and *pstC*) (4). The roles of peptide synthetase may be modified by an N-acylated Phe acceptor by sequential addition of Thr, Ala, and alaninol residues by peptidosynthetase, encoded by *mps*. This lipopeptide core may subsequently be glycosylated with rhamnose and 6-deoxy talose, resulting in the nonspecific core GPL that is found in all members of *M. avium* as well as *M. smegmatis* (3). The nsGPLs are further elaborated with oligosaccharide structures to produce the antigenically important serovar-specific GPLs (5). *M. smegmatis*, which produces only nsGPL, has been used to identify the genes for the glycosyltransferase and methyltransferase involved in elaborating the nsGPL with the hepatenic oligosaccharides of *M. avium* serovar 2 (11, 21). Furthermore, the *M. avium* A5 transposon mutant of 4B2 obtained in the present study had the *pstB* gene inactivated, which was encoded in the sequences of the GPL biosynthesis gene cluster and daunorubicine gene in *M. avium* 2151 (GenBank accession no. AF143772) (4).

The role that mycolic acid plays in mycobacterial biofilm formation is unclear. Polyketide synthetase is responsible for the synthesis of methyl-branched fatty acids in *M. tuberculosis*. Analysis of the *M. tuberculosis* genome sequence has revealed the existence of several polyketide synthases (*pks*) (29). In an attempt to determinate the function of mycobacterial *pks*, mutants deficient in the expression of the pks10 and ppsB/ppsC, pks2, pks3/4, pks10, and pks15/1 genes were constructed by allelic replacement in *M. tuberculosis* or *M. bovis* BCG. The *pks* gene, disruption of which in *M. tuberculosis* H37Rv also caused dimycocerosate deficiency without affecting the ability of the mutant strain to synthesize mycocerosic acids, is thought to be involved in the production of phthiocerol derivatives (14, 31). The precise function of *pks10* is currently unclear. Recent work suggests that polyketides are important in the ability of *M. tuberculosis* to prevent activation of the innate immunoresponse (27), but its role in the formation of biofilm will need further investigation.

The transposon library of *M. avium* strain A5, screened for the identification of clones with an impaired ability to produce biofilm on PVC, led to the identification of five clones (four genes). The transposon mutant clone, 6H9, has the gene homologue of 2-oxoglutarate dehydrogenase (*OX*) in the TCA cycle inactivated. The conversion of propionyl-CoA and succinyl-CoA leads to succinate and malate in the TCA cycle (16). It has been reported for *Salmonella enteritidis* that *sucD*, the succinyl-CoA synthetase alpha subunit and an enzyme upstream of 2-oxodehydrogenase, has been identified as an important enzyme in the formation of biofilm by the bacterium (33). The mutants 6H9 and 4B2 encode *sucA* and *pstB*, which are associated with GPL synthetase. The gene inactivated in the 5G4 mutant was highly homologous to *M. tuberculosis* genomic Rv1565c, a hypothetical membrane protein. It is located upstream of the trehalose synthetase genes *treX*, *treY*, and *treZ*. These genes encode malto-oligosyltrehalose synthase, malto-oligosyltrehalose synthase, and malto-oligosyltrehalose, respectively, which are well conserved between the *M. tuberculosis* and *M. avium* 104 genomes. In *M. tuberculosis*, trehalose has been known to participate in mycolic acid synthesis; mycolic acids are complemented by glycolipids such as a,a′-trehalose dimycolate and a,a′-trehalose monomycolate (5). The 9B5 clone of *M. avium* A5 has the *pcd* gene inactivated. The *pcd* gene encoding P6CDH (Rv3293) is involved in the biosynthesis of α aminoadipic acid. It is located in the cephamycin C gene cluster of *Streptomyces clavuligerus* (1, 25). P6CDH, which converts 1-piperideine-6-carboxylic acid into α aminoadipic acid, a precursor of cephamycin C, has recently

been purified (10). Since there was no cephamycin C gene cluster around the *pcd* gene in the mycobacterial genome, it is not easy to explain the roles of P6CDH with biofilm formation or GPL biosynthesis in *M. avium*. The complemented strains of both 5G4 and 9B5 restored the ability of the strains to form biofilms.

In summary, work with the strain A5 identified several genes associated with biofilm formation. Most of genes are involved in GPL biosynthesis, which indicates that the outer surface of the bacterium is likely to be important for the establishment of biofilm. The future aim of this work is to find a regulator(s) for the formation of biofilm.

ACKNOWLEDGMENTS

We are grateful to Denny Weber for editing the manuscript.

This work was supported by a grant of the National Institute of Allergy and Infectious Diseases (AI-43199).

REFERENCES

1. **Alexander, D. C., and S. E. Jensen.** 1998. Investigation of the *Streptomyces clavuligerus* cephamycin C gene cluster and its regulation by the CcaR protein. J. Bacteriol. **180:**4068–4079.
2. **Beggs, M. L., J. T. Crawford, and K. D. Eisenach.** 1995. Isolation and sequencing of the replication region of *Mycobacterium avium* plasmid pLR7. J. Bacteriol. **177:**4836–4840.
3. **Belisle, J. T., and P. J. Brennan.** 1989. Chemical basis of rough and smooth variation in mycobacteria. J. Bacteriol. **171:**3465–3470.
4. **Billman-Jacobe, H., M. J. McConville, R. E. Haites, S. Kovacevic, and R. L. Coppel.** 1999. Identification of a peptide synthetase involved in the biosynthesis of glycopeptidolipids of *Mycobacterium smegmatis*. Mol. Microbiol. **33:**1244–1253.
5. **Brennan, P. J., and H. Nikaido.** 1995. The envelope of mycobacteria. Annu. Rev. Biochem. **64:**29–63.
6. **Carter, G., M. Wu, D. C. Drummond, and L. E. Bermudez.** 2003. Characterization of biofilm formation by clinical isolates of *Mycobacterium avium*. J. Med. Microbiol. **52:**747–752.
7. **Chatterjee, D., and K. H. Khoo.** 1998. *Mycobacterial lipoarabinomannan*: an extraordinary lipoheteroglycan with profound physiological effects. Glycobiology **8:**113–120.
8. **Costerton, W., R. Veeh, M. Shirtliff, M. Pasmore, C. Post, and G. Ehrlich.** 2003. The application of biofilm science to the study and control of chronic bacterial infections. J. Clin. Investig. **112:**1466–1477.
9. **Danelishvili, L., M. J. Poort, and L. E. Bermudez.** 2004. Identification of *Mycobacterium avium* genes up-regulated in cultured macrophages and in mice. FEMS Microbiol. Lett. **239:**41–49.
10. **de La Fuente, J. L., A. Rumbero, J. F. Martin, and P. Liras.** 1997. Delta-1-piperideine-6-carboxylate dehydrogenase, a new enzyme that forms alpha-aminoadipate in *Streptomyces clavuligerus* and other cephamycin C-producing actinomycetes. Biochem. J. **327:**59–64.
11. **Eckstein, T. M., J. M. Inamine, M. L. Lambert, and J. T. Belisle.** 2000. A genetic mechanism for deletion of the *ser2* gene cluster and formation of rough morphological variants of *Mycobacterium avium*. J. Bacteriol. **182:** 6177–6182.
12. **Guilhot, C., I. Otal, I. Van Rompaey, C. Martin, and B. Gicquel.** 1994. Efficient transposition in mycobacteria: construction of *Mycobacterium smegmatis* insertional mutant libraries. J. Bacteriol. **176:**535–539.
13. **Kang, B. K., and L. S. Schlesinger.** 1998. Characterization of mannose receptor-dependent phagocytosis mediated by *Mycobacterium tuberculosis* lipoarabinomannan. Infect. Immun. **66:**2769–2777.
14. **Kolattukudy, P. E., N. D. Fernandes, A. K. Azad, A. M. Fitzmaurice, and T. D. Sirakova.** 1997. Biochemistry and molecular genetics of cell-wall lipid biosynthesis in mycobacteria. Mol. Microbiol. **24:**263–270.
15. **Kordulakova, J., M. Gilleron, K. Mikusova, G. Puzo, P. J. Brennan, B. Gicquel, and M. Jackson.** 2002. Definition of the first mannosylation step in phosphatidylinositol mannoside synthesis. PimA is essential for growth of mycobacteria. J. Biol. Chem. **277:**31335–31344.
16. **Korotkova, N., L. Chistoserdova, V. Kuksa, and M. E. Lidstrom.** 2002. Glyoxylate regeneration pathway in the methylotroph *Methylobacterium extorquens* AM1. J. Bacteriol. **184:**1750–1758.
17. **Krzywinska, E., and J. S. Schorey.** 2003. Characterization of genetic differences between *Mycobacterium avium* subsp. *avium* strains of diverse virulence with a focus on the glycopeptidolipid biosynthesis cluster. Vet. Microbiol. **91:**249–264.
18. **Li, Y., E. Miltner, M. Wu, M. Petrofsky, and L. E. Bermudez.** 2005. A *Mycobacterium avium* PPE gene is associated with the ability of the bacterium to grow in macrophages and virulence in mice. Cell Microbiol. **7:**539–548.
19. **Martinez, A., S. Torello, and R. Kolter.** 1999. Sliding motility in mycobacteria. J. Bacteriol. **181:**7331–7338.
20. **Menon, S., M. Stahl, R. Kumar, G. Y. Xu, and F. Sullivan.** 1999. Stereochemical course and steady state mechanism of the reaction catalyzed by the GDP-fucose synthetase from *Escherichia coli*. J. Biol. Chem. **274:**26743–26750.
21. **Mills, J. A., M. R. McNeil, J. T. Belisle, W. R. Jacobs, Jr., and P. J. Brennan.** 1994. Loci of *Mycobacterium avium ser2* gene cluster and their functions. J. Bacteriol. **176:**4803–4808.
22. **Mukhopadhyay, B., E. M. Concar, and R. S. Wolfe.** 2001. A GTP-dependent vertebrate-type phosphoenolpyruvate carboxykinase from *Mycobacterium smegmatis*. J. Biol. Chem. **276:**16137–16145.
23. **Nigou, J., M. Gilleron, M. Rojas, L. F. Garcia, M. Thurnher, and G. Puzo.** 2002. Mycobacterial lipoarabinomannans: modulators of dendritic cell function and the apoptotic response. Microbes Infect. **4:**945–953.
24. **Ortalo-Magne, A., A. Lemassu, M. A. Laneelle, F. Bardou, G. Silve, P. Gounon, G. Marchal, and M. Daffe.** 1996. Identification of the surface-exposed lipids on the cell envelopes of *Mycobacterium tuberculosis* and other mycobacterial species. J. Bacteriol. **178:**456–461.
25. **Perez-Llarena, F. J., A. Rodriguez-Garcia, F. J. Enguita, J. F. Martin, and P. Liras.** 1998. The *pcd* gene encoding piperideine-6-carboxylate dehydrogenase involved in biosynthesis of alpha-aminoadipic acid is located in the cephamycin cluster of *Streptomyces clavuligerus*. J. Bacteriol. **180:**4753–4756.
26. **Recht, J., and R. Kolter.** 2001. Glycopeptidolipid acetylation affects sliding motility and biofilm formation in *Mycobacterium smegmatis*. J. Bacteriol. **183:**5718–5724.
27. **Reed, M. B., P. Domenech, C. Manca, H. Su, A. K. Barczak, B. N. Kreiswirth, G. Kaplan, and C. E. Barry III.** 2004. A glycolipid of hypervirulent tuberculosis strains that inhibits the innate immune response. Nature **431:**84–87.
28. **Rosenzweig, D. Y.** 1979. Pulmonary mycobacterial infections due to *Mycobacterium intracellulare-avium* complex. Clinical features and course in 100 consecutive cases. Chest **75:**115–119.
29. **Rousseau, C., T. D. Sirakova, V. S. Dubey, Y. Bordat, P. E. Kolattukudy, B. Gicquel, and M. Jackson.** 2003. Virulence attenuation of two Mas-like polyketide synthase mutants of *Mycobacterium tuberculosis*. Microbiology **149:**1837–1847.
30. **Schlesinger, L. S., S. R. Hull, and T. M. Kaufman.** 1994. Binding of the terminal mannosyl units of lipoarabinomannan from a virulent strain of *Mycobacterium tuberculosis* to human macrophages. J. Immunol. **152:**4070–4079.
31. **Sirakova, T. D., V. S. Dubey, H. J. Kim, M. H. Cynamon, and P. E. Kolattukudy.** 2003. The largest open reading frame (pks12) in the *Mycobacterium tuberculosis* genome is involved in pathogenesis and dimycocerosyl phthiocerol synthesis. Infect Immun. **71:**3794–3801.
32. **Snapper, S. B., R. E. Melton, S. Mustafa, T. Kieser, and W. R. Jacobs, Jr.** 1990. Isolation and characterization of efficient plasmid transformation mutants of *Mycobacterium smegmatis*. Mol. Microbiol. **4:**1911–1919.
33. **Solano, C., B. Garcia, J. Valle, C. Berasain, J. M. Ghigo, C. Gamazo, and I. Lasa.** 2002. Genetic analysis of *Salmonella enteritidis* biofilm formation: critical role of cellulose. Mol. Microbiol. **43:**793–808.
34. **Stevenson, G., K. Andrianopoulos, M. Hobbs, and P. R. Reeves.** 1996. Organization of the *Escherichia coli* K-12 gene cluster responsible for production of the extracellular polysaccharide colanic acid. J. Bacteriol. **178:**4885–4893.
35. **Van Dien, S. J., Y. Okubo, M. T. Hough, N. Korotkova, T. Taitano, and M. E. Lidstrom.** 2003. Reconstruction of C(3) and C(4) metabolism in *Methylobacterium extorquens* AM1 using transposon mutagenesis. Microbiology **149:** 601–609.
36. **von Reyn, C. F., J. N. Maslow, T. W. Barber, J. O. Falkinham III, and R. D. Arbeit.** 1994. Persistent colonisation of potable water as a source of *Mycobacterium avium* infection in AIDS. Lancet **343:**1137–1141.

研究成果の刊行に関する一覧表

雑誌

発表者氏名	論文タイトル名	発表誌名	巻号	ページ	出版年
永井英明	HIV感染症合併結核	日本医事新報	4287	64-67	2006
永井英明	結核合併例の治療ストラテジー	診断と治療	94	2273-2276	2006
永井英明	結核の診断と治療	治療	88	2951-2954	2006
永井英明	ニューモシスチス肺炎	内科	97	1204-1205	2006
川辺　芳子	クォンティフェロン®TB第2世代による結核感染の診断	呼吸	25	490-495	2006
永井英明	結核ー多剤耐性結核を防ぐ新治療基準	NURSE SENKA	26	82-85	2006

特集　あなどれない結核

HIV感染症合併結核

国立病院機構東京病院呼吸器科医長
永井（ながい）　英明（ひであき）

【要　旨】
日本の結核罹患率は高く、HIV感染者も増加傾向にある。今後は、HIV感染症合併結核例が増加する可能性がある。両者の治療を同時に行う場合は、副作用、薬剤相互作用、免疫再構築症候群などを考慮しなければならない。

□はじめに

日本の結核の罹患率は結核対策により減少し、2004年の結核罹患率は人口10万対23・3となったが、欧米先進国の結核罹患率が10以下であることを思えば、日本は結核では中進国である。また、HIV感染・AIDS患者数は増加傾向にあり、2005年には2年連続で1000名を超えた。このような状況の日本では、今後HIV感染症合併結核の症例が増加する可能性がある。森ら[1]によると、2001年12月末までに222例の結核を合併したHIV感染者が確認されており、年々増加している。当院でも両者合併例は1992年以来徐々に増加し[2]、2005年末までに55例を経験している。

結核患者におけるHIV感染症の合併頻度については、全国レベルの調査はないが当院の症例について調べたところ[3]、抗HIV抗体陽性率は結核患者全体では3・2%、HIV感染症が疑われなかった症例では1・0%、粟粒結核では28・6%と高率であった。しかし、このデータは結核患者もHIV感染者も多い東京地区のデータであることを認識しておかなければならない。

今後も、HIV感染症に合併した結核の増加が予想されるので、臨床の現場では注意が必要である。

□HIV感染症における結核発病のリスク

HIVは主にCD4陽性Tリンパ球（CD4）に感染し、その細胞数が極端に減少することにより重篤な細胞性免疫障害が生じる。CD4の障害はさらにマクロファージ機能（抗原提示能、遊走能、活性化）の障害をもたらす。結核の感染防御に最も重要な働きを示すのは、CD4とマクロファージである。

したがって、これらの細胞の機能障害が生じるHIV感染症においては、結核に感染し発病しやすい。細胞性免疫が低下した状態で結核を発病すると、肉芽腫の形成不全、結核菌の抑制不全、大量の結核菌による頻回の再燃、局所リンパ節への波及（肺門、縦隔リンパ節）、血行性の全身播種が起こりうる。この場合においては、乾酪性壊死と空洞形成は起こりにくくなる。

非HIV感染者が結核に感染した場合、結核が発病する確率は一生涯に5～10%といわれているが、HIV感染者が結核に感染した場合は、その発病する率は年間5～10%といわれ高率であり、その50%は2年以内に発病するといわれている[4]。

□臨床像

結核菌はHIV感染症に合併する日和見感染症を引き起こす病原体の中では比較的強毒性のため、結核症は早期（CD4数300～400 μℓ）から合併しやすい。症状は、発熱、倦怠感、体重減少、盗汗、咳嗽、喀痰などで、非HIV感染者の結核と同様であるが、他の日和見感染症にもみられる症状である。進行が速い場合があるので早期発見が重要である。ツベルクリン反応（ツ反応）は免疫能低下のため陰性であることが多い。

胸部X線写真では、免疫能が比較的保たれている時期では、肺尖部に空洞形成を伴う典型的な像を呈する。しかし、免疫能が低下した時期では、下葉の病変、非空洞形成、肺門・縦隔のリンパ節腫脹、粟粒影など非典型像を認めるようになる（図1）。

HIV感染症に合併した結核では、肺外結核の頻度が高いのが特徴である。肺外結核としては、リンパ節結核および播種型が最も多い。ほかに消化管、泌尿生殖器、中枢神経系における結核もしばしばみられる。HIV感染者では非HIV感染者に比較し、2倍の頻度で肺外結核を合併するといわれている。またHIV感染者の中でも、肺外結核を合併した症例は、合併しない症例よりもCD4数が低値である。

isoniazid（INH）・rifampicin（RFP）両剤耐性を含む耐性結核菌を多剤耐性菌というが、HIV感染者に多剤耐性菌感染が生じた場合は、きわめて予後が不良である。

□診　断

結核の罹患率の高いわが国では、HIV感染者に胸部異常影を認めた場合は常に結核の合併を念頭に置き、結核菌の検索を行うべきである。血液培養での結核菌の検出は、非HIV感染者の結核では稀であるが、HIV感染者の結核ではしばしば認められる。

□強力な抗HIV療法時代におけるAIDSと結核

強力な抗HIV療法（highly active antiretroviral therapy：HAART）が導入されてからHIV感染症の予後は著明に改善し、AIDS関連疾患の減少とHIV感染者の死亡率の減少が認められている[5)～7)]。また、HAARTはHIV感染症における活動性結核の合併リスクを減少させたという報告[8)9)]もみられる。

HIV感染症合併結核症例に対して、HAARTを行うことにより予後の改善が得られたかという点についての報告は今のところ多くない。Girardis[8)]によれば、HIV感染症合併結核症例に対して抗HIV療法を行わなかったか、あるいは抗HIV薬を1剤しか投与しなかった群の死亡についてのhazard ratioを1とした場合、抗HIV薬を3剤投与した群では0・14であり、有効なHAARTを行った場合、HIV感染症合併結核例の生存率は著明に改善したという。しかし、すでにHAARTを行っていた患者に結核が合併した場合は、むしろ予後不良であったとのことである。

□HIV感染症合併結核の治療上の問題点

HIV感染症合併結核の治療を行う上で注意すべき点としては、主に以下の3点がある。

(1)薬剤の副反応が起こりやすい

HIV感染症では薬剤の副反応が起こりやすく、細心の注意を払う必要がある。特に、抗結核薬では皮疹と肝障害の副作用が多い。抗結核薬と抗HIV薬を同時に内服する場合は両者の副反応を生じる可能性が高く、原因薬剤の同定が困難となるだけでなく、すべての治療を中断せざるをえない状況に追い込まれることがある。

(2)rifamycin系薬剤と抗HIV薬との間に薬剤相互作用がある

rifamycin系薬剤（RFP、rifabutin, rifapentine）は、肝臓と腸管においてcytochrome P450（特にCYP3A4）の誘導作用が強い。CYP3A4により代謝されるプロテアーゼ阻害薬や非核酸系逆転写酵素阻害薬の血中濃度は、rifamycin系薬剤と併用することにより著しく低下し、抗HIV作用は低下する。また、逆にプロテアーゼ阻害薬は強力なCYP3A4抑制作用を持つ。このような理由から、プロテアーゼ阻害薬お

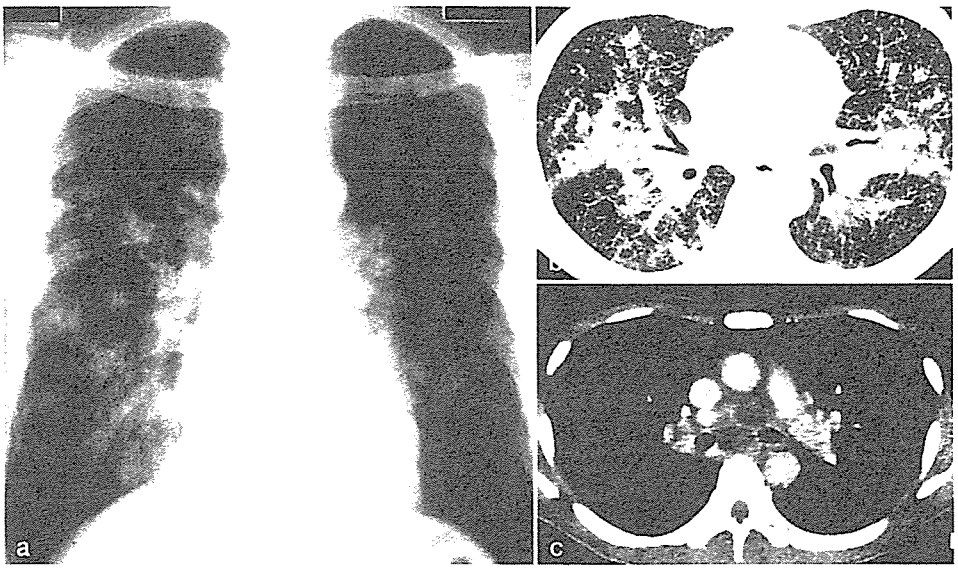

図1　30歳代のAIDS合併粟粒結核患者のX線写真とCT

胸部単純X線写真(a)では，両肺びまん性の粟粒影と両側中肺野を中心とする浸潤影，多発小結節影，縦隔リンパ節の腫脹を認めた．

CT(b･c)では，粟粒影，多発小結節影，気管支周囲の浸潤影および縦隔リンパ節の腫脹を認めた．縦隔リンパ節は辺縁が造影され，内部は壊死様である．

よび非核酸系逆転写酵素阻害薬とRFPとの併用は注意が必要である。

結核の治療中に前記2系統の抗HIV薬を開始する場合は、RFPよりもCYP3A4の誘導が弱いrifabutin〔わが国では承認されておらず、エイズ治療薬研究班(東京医科大学臨床病理科)より譲り受ける〕を用いることが多かったが、米国のCDC(疾病予防センター)[10]はRFPとritonavir, ritonavir+saquinavir, efavirenzとの併用を可能としたため、選択肢が増えた。

当院ではRFPとefavirenzの併用を行っているが、efavirenzの血中濃度の測定を行い、有効性を確認している。

(3)免疫再構築症候群が起こることがある

結核治療中に早期にHAARTを開始した場合、結核の一時的悪化をみることがある[11]。症状・所見としては高熱、リンパ節腫脹、胸部X線所見の悪化(肺野病変および胸水の増悪)などがみられる。この反応は、細胞性免疫能が回復し、生体側の反応が強くなったために引き起こされると考えられており、免疫再構築症候群といわれている。

免疫再構築症候群と診断された場合は抗結核薬の変更は必要ないが、症状が強い場合は抗炎症剤や短期の副腎皮質ステロイドの投与、重症例では抗HIV薬の中止が必要になることがある。

□HIV感染症合併結核の治療

感受性菌であれば、非HIV感染者における結核と同様に抗結核薬によく反応する。治療法としては、INH、RFP、pyrazinamide, ethambutol(EB)(あるいはstreptomycin)の4剤を2カ月間投与し、その後INH、RFPの2剤(あるいはEBを加えた3剤)を4カ月継続して、全治療期間を6カ月間とする、いわゆる短期療法でよいとされている[12]。しかし、臨床的に効果の遅い症例や3カ月以上結核菌の喀痰培養が陽性の症例では、治療期間を延長すべきである。

多剤耐性菌の場合はきわめて予後不良であり、死亡率が高い。感